SAND2022-14732C

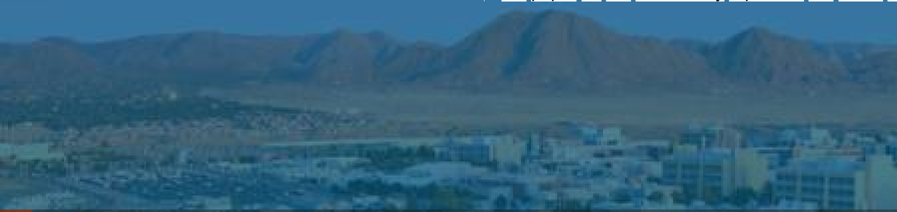

Small-Scale Reconsolidation Studies

PRESENTED BY

Ed Matteo (SNL - org. 8842)

Team: Tom Dewers, Melissa Mills, Ben Reedlunn (SNL)

Rob Lander, Linda Bonell, and Jim Guilkey (GEOCOSM, LLC)

John Stormont, Benjamin Gallego, and Evan Babcock (UNM)

Sandia National Laboratories is a multimission laboratory managed and operated by National Technology & Engineering Solutions of Sandia, LLC, a wholly owned subsidiary of Honeywell International Inc., for the U.S. Department of Energy's National Nuclear Security Administration under contract DE-NA0003525. This research is funded by WIPP programs by the Office of Environmental Management (EM) of the U.S. Department of Energy.
SAND #:

Sandia National Laboratories is a multimission laboratory managed and operated by National Technology & Engineering Solutions of Sandia, LLC, a wholly owned subsidiary of Honeywell International Inc., for the U.S. Department of Energy's National Nuclear Security Administration under contract DE-NA0003525.

Overview

Overview of the Research Strategy

Highlights from Activities

- We have used computational tools to simulate many rubble pile packings, courtesy of GEOCOSM, both monodisperse and polydisperse, including salt shape geometries and spheres (for sanity check and comparison).
- Preliminary experimental tests on polydisperse salt rubble piles (at 1:10 scale)
- Development of CFD analysis of the GEOCOSM packings (to construct porosity permeability relationships), as well as perform validation tests on the 1:10 scale salt piles while measuring permeability and porosity (and verifying the porosity measurement via micro CT).
- In progress:
  - CFD of GEOCOSM packs
  - Validation tests, using micro CT at SNL – post-test data processing underway
  - Computational compaction of GEOCOSM rubble piles

Summary and Conclusions

Research Strategy

1. Generate synthetic rubble pile realizations
    1. Verify approach using monodisperse spherical packs
    2. Vary clast shapes and size distributions
2. Simulate compaction with various levels of sophistication
3. Use CFD to compute permeability
    1. Explicitly represent macroflow channels and implicitly represent microflow channels
4. Validate against crushed salt or small-scale rubble compaction experiments
    1. Vary the grain size distribution, temperature, and compaction pressure

Synthetic Rubble Pile

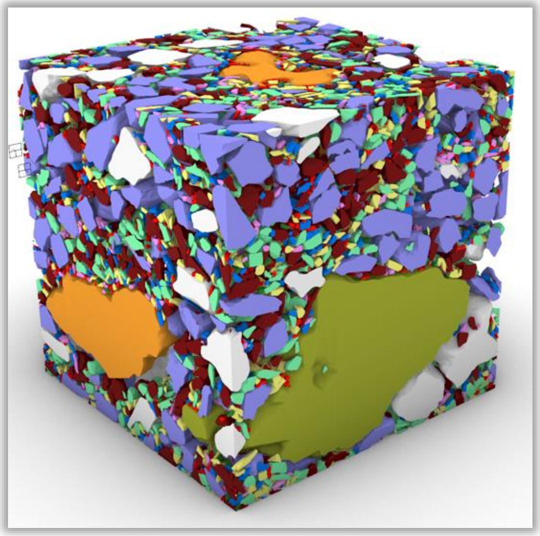

<u>Expected outcomes</u> - understanding of sensitivities to particle size distributions (esp. polydispersity), but also particle shape geometries

Workflow and Coordinating Interfaces between SNL, Geocosm, and UNM Teams

Project Start 2018

1. Characterization of rubble size and shape using X-ray micro-computed tomography
2. Image analysis to include solid segmentation and grain separation, using a variety of filters and watershed methods. *(This did not work!)*
3. Particle Shape Geometries via Sieve Analysis on ROM Salt

June 2020

4. Creation of grain size distributions of rubble piles
5. Creation of grain surface meshes extracted from the separated particles, using the distribution as a guide.
6. Cyberstone modeling of rubble consolidation, extracting representative shapes and sizes using the provided STL files and the resulting volume distribution as a guide.

Oct. 2022

7. CFD modeling of gas transport in the consolidating rubble piles from the Cyberstone results.
8. Validation against UNM 1:10 scale experiments

DEPOSITION SIMULATIONS

Clast Deposition Simulations

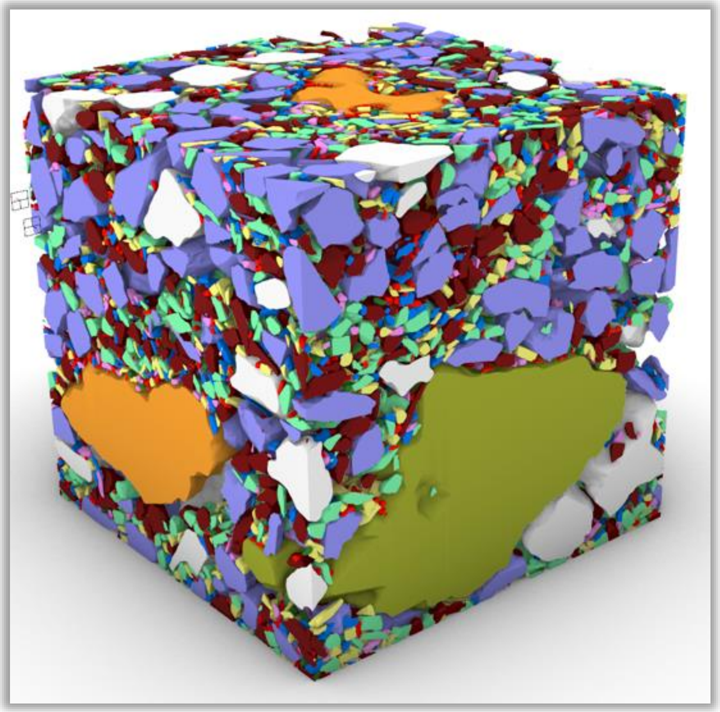

Vetting results ("Sanity" checks)
- Angle of repose simulations
- Sphere packs with uniform sizes

Deposition simulations
- "Gentle" vs. "Mass Dump" results
- Shaking and low friction
- Uniform size vs. sieve size distribution
- Spheres vs. μCT based shapes

Cyberstone Angle of Repose Simulations (Sanity Check #1)

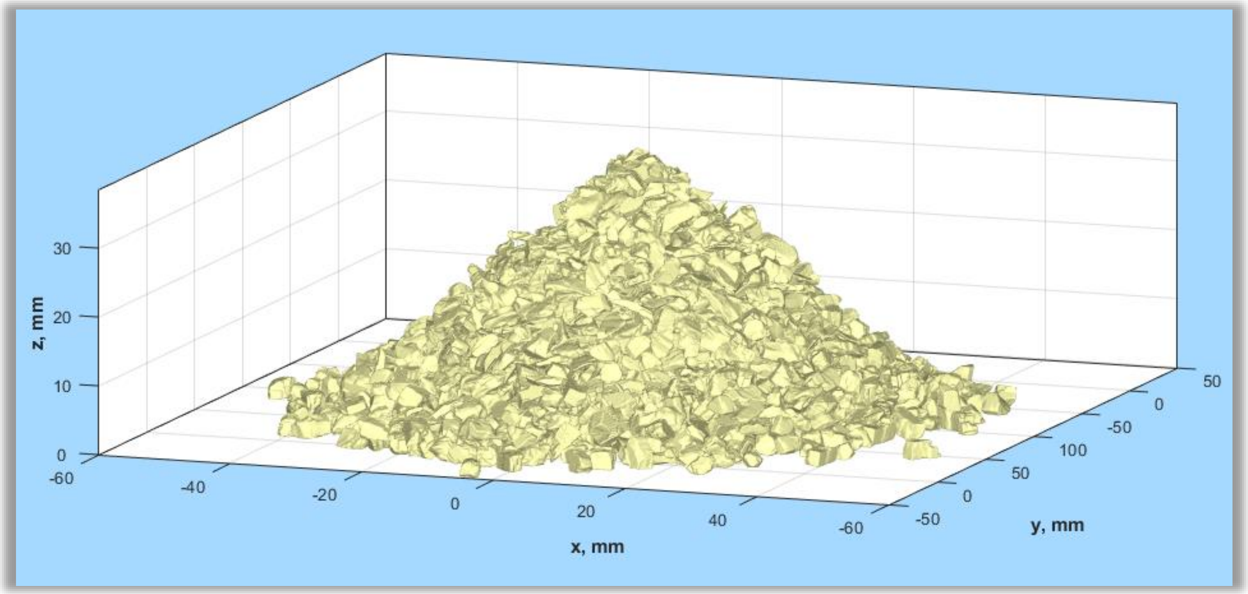

Drop clasts from same x/y position at a constant height above the top of the sediment pile

Use same friction values for floor as for clasts

Angles of Repose: UNM and Cyberstone

Angle of repose measurement with granular salt from WIPP
University of New Mexico
April 23, 2021

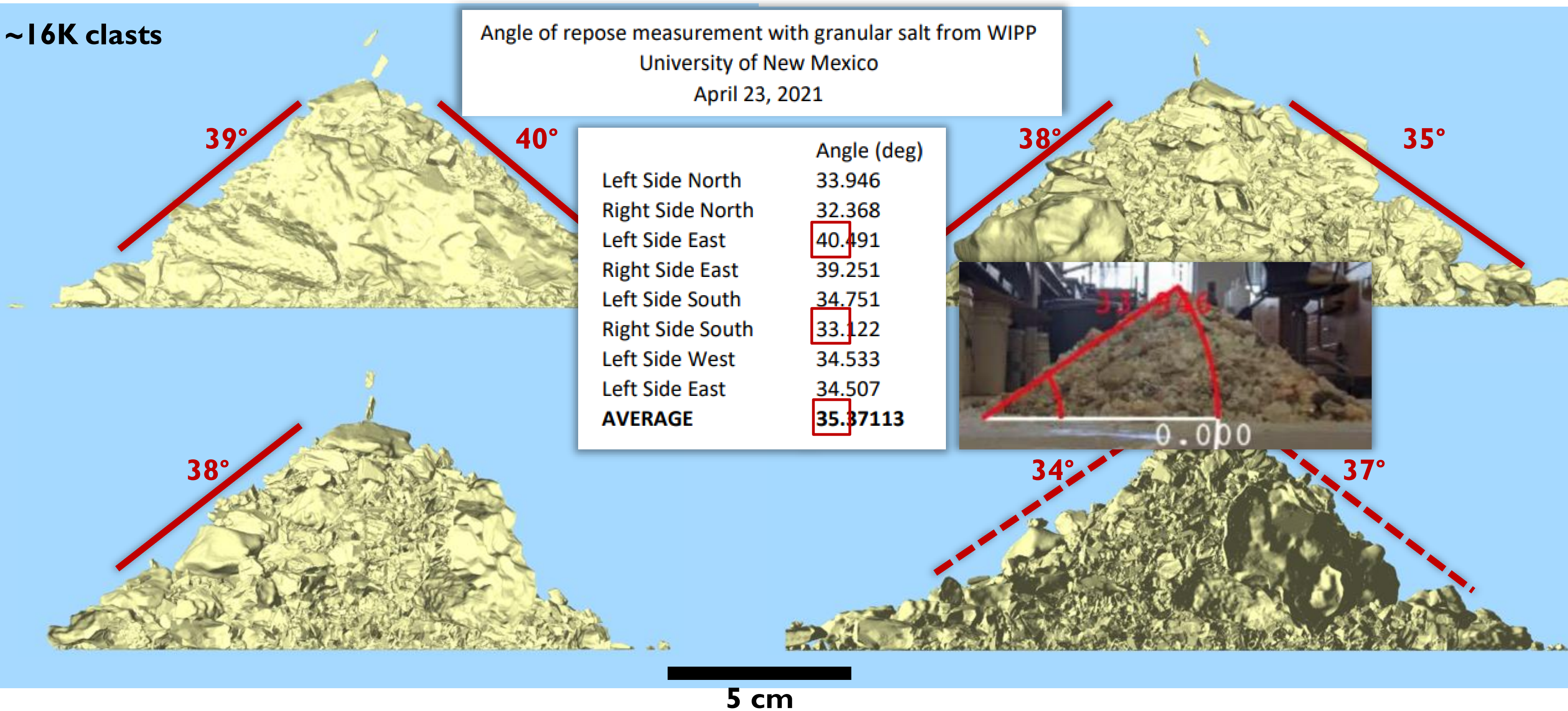

	Angle (deg)
Left Side North	33.946
Right Side North	32.368
Left Side East	40.491
Right Side East	39.251
Left Side South	34.751
Right Side South	33.122
Left Side West	34.533
Left Side East	34.507
AVERAGE	**35.37113**

Uniform (Monodisperse) Sphere Simulations (“Sanity Check” #2)

μ 0.10 + shaking: Porosity 36.4 vol%

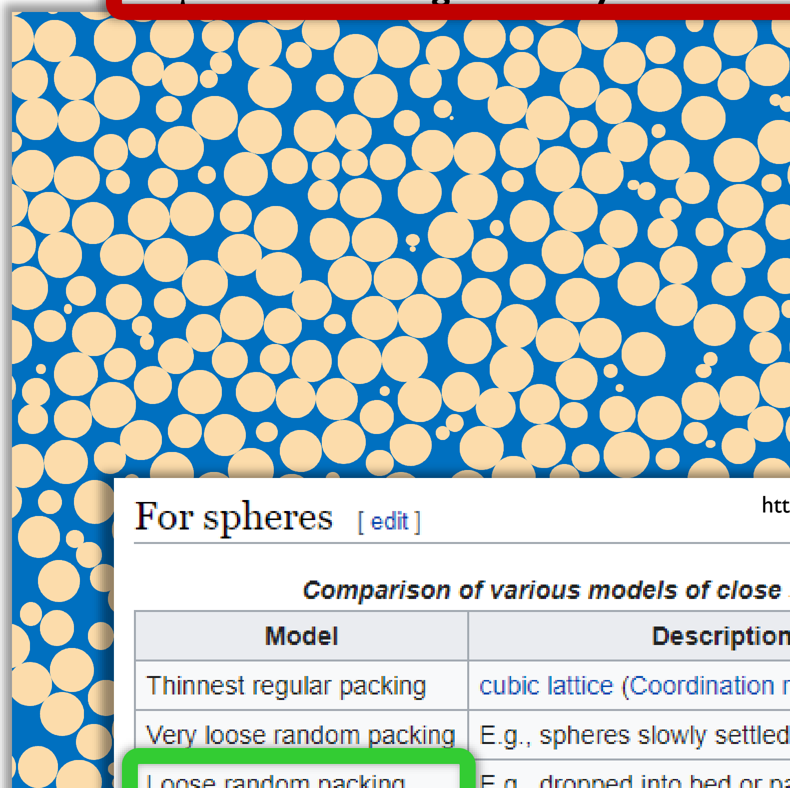

μ 0.77: Porosity 40.4 vol

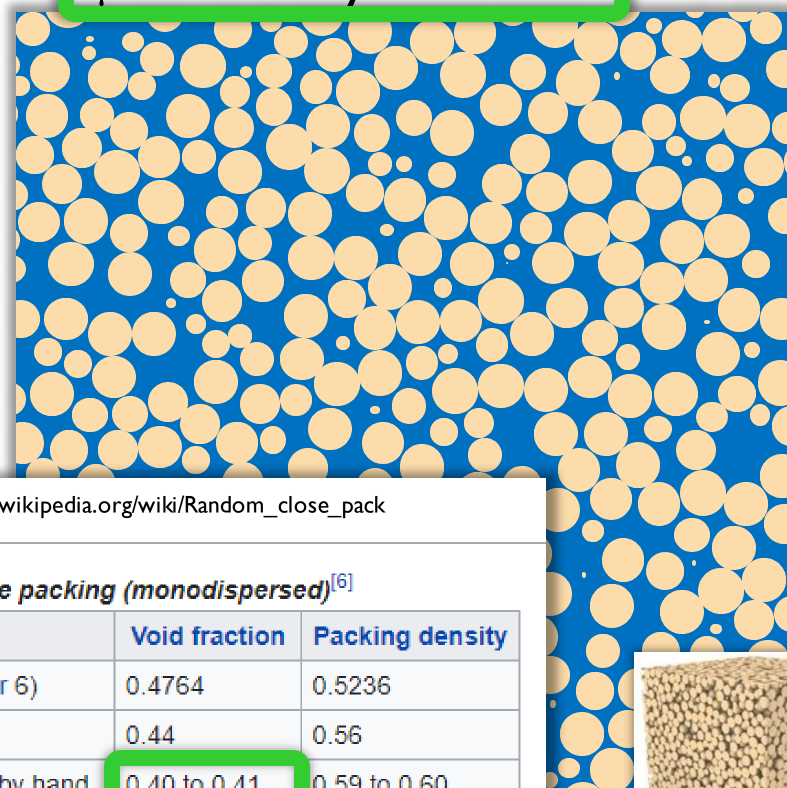

For spheres [edit]

https://en.wikipedia.org/wiki/Random_close_pack

Comparison of various models of close sphere packing (monodispersed)[6]

Model	Description	Void fraction	Packing density
Thinnest regular packing	cubic lattice (Coordination number 6)	0.4764	0.5236
Very loose random packing	E.g., spheres slowly settled	0.44	0.56
Loose random packing	E.g., dropped into bed or packed by hand	0.40 to 0.41	0.59 to 0.60
Poured random packing	Spheres poured into bed	0.375 to 0.391	0.609 to 0.625
Close random packing	E.g., the bed vibrated	0.359 to 0.375	0.625 to 0.641
Densest regular packing	fcc or hcp lattice (Coordination number 12)	0.2595	0.7405

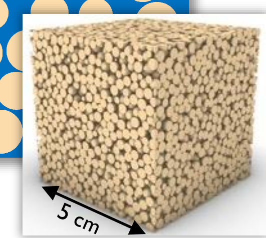

Rubble Deposition Simulations: μCT Shapes

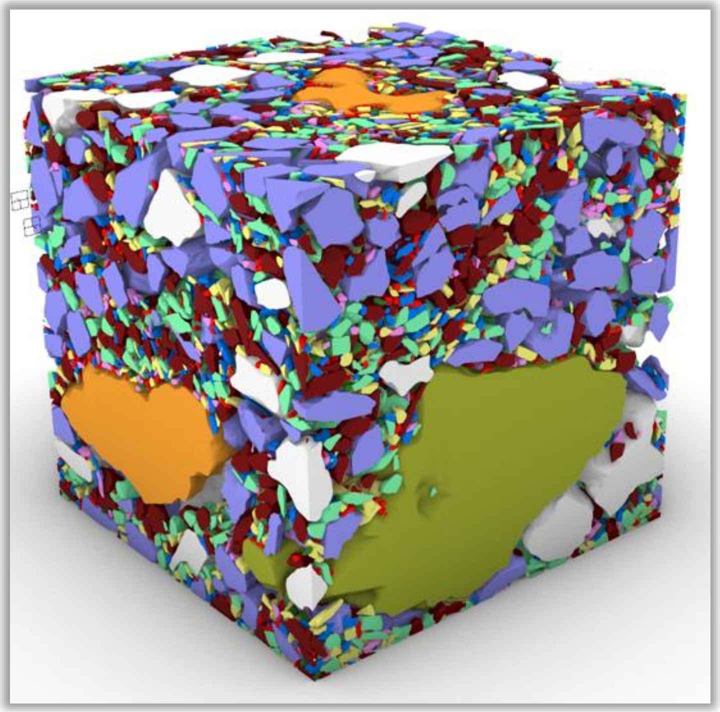

Variables

- Mass dump vs. gentle deposition
- Friction coefficient
- Shaking

Alternative Rubble Deposition Modes

	Opening, mm		
	Min	Max	Color
Sieve A	38.1	57.2	
Sieve B	19.1	28.6	
Sieve C	9.5	14.3	
Sieve 4	4.7	7.1	
Sieve 6	3.4	4.1	
Sieve 8	2.4	2.9	
Sieve 10	2.0	2.2	
Sieve 12	1.7	1.8	
Sieve 14	1.4	1.5	
Sieve 16	1.2	1.3	
Sieve 18	1.0	1.1	

POROSITY RESULTS

- Gentle: 37.4%
- Mass Dump: 37.0%

"Gentle"

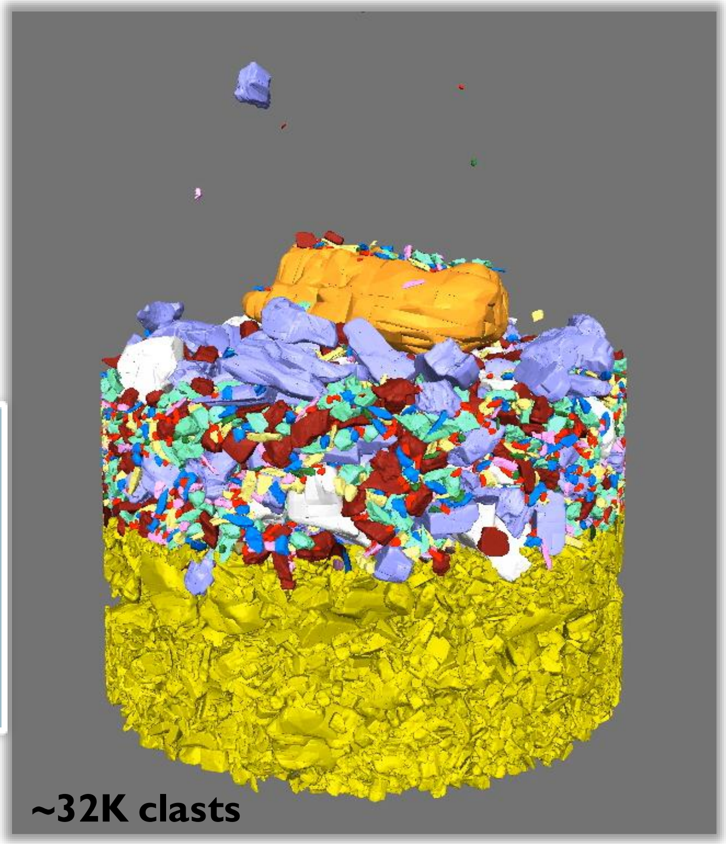

"Mass Dump"

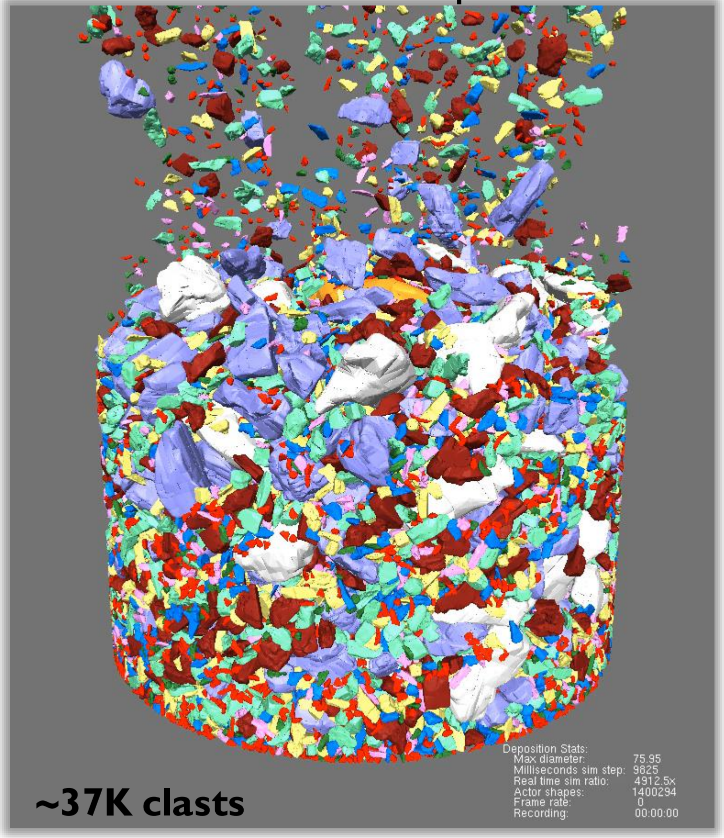

Shaking with Same Friction (μ = 0.77)

Porosity 37.0 vol%

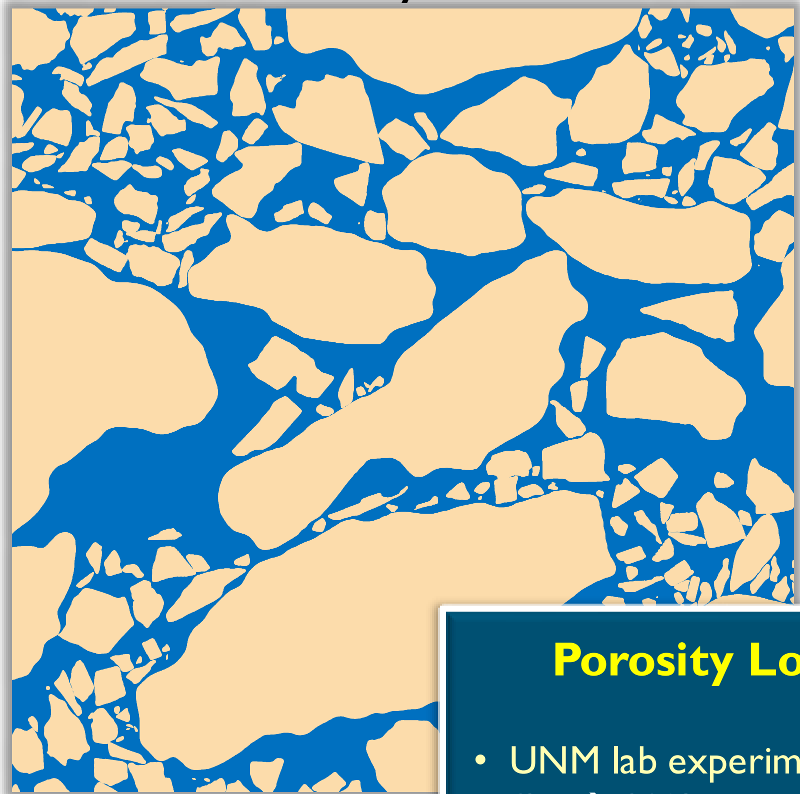

Porosity 33.6 vol% after shaking

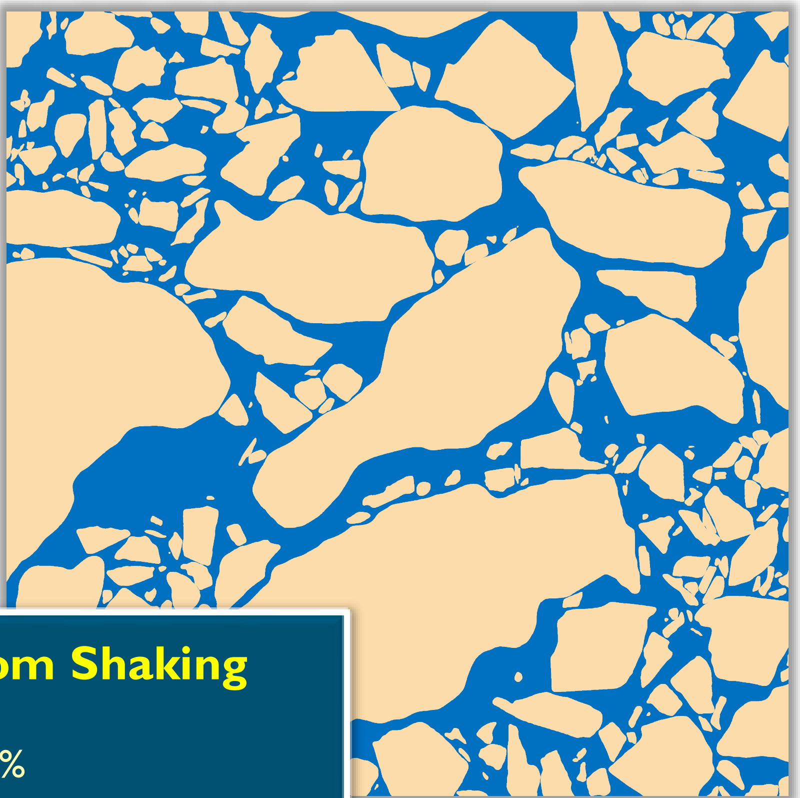

Porosity Loss from Shaking

- UNM lab experiment ~3% (35 → 32% porosity, J. Stormont, pers comm)
- Cyberstone simulation ~3.4%

Sieve Size Distribution: Impact of Shaking + Low Friction

Porosity 37.0 vol% (μ = 0.77)

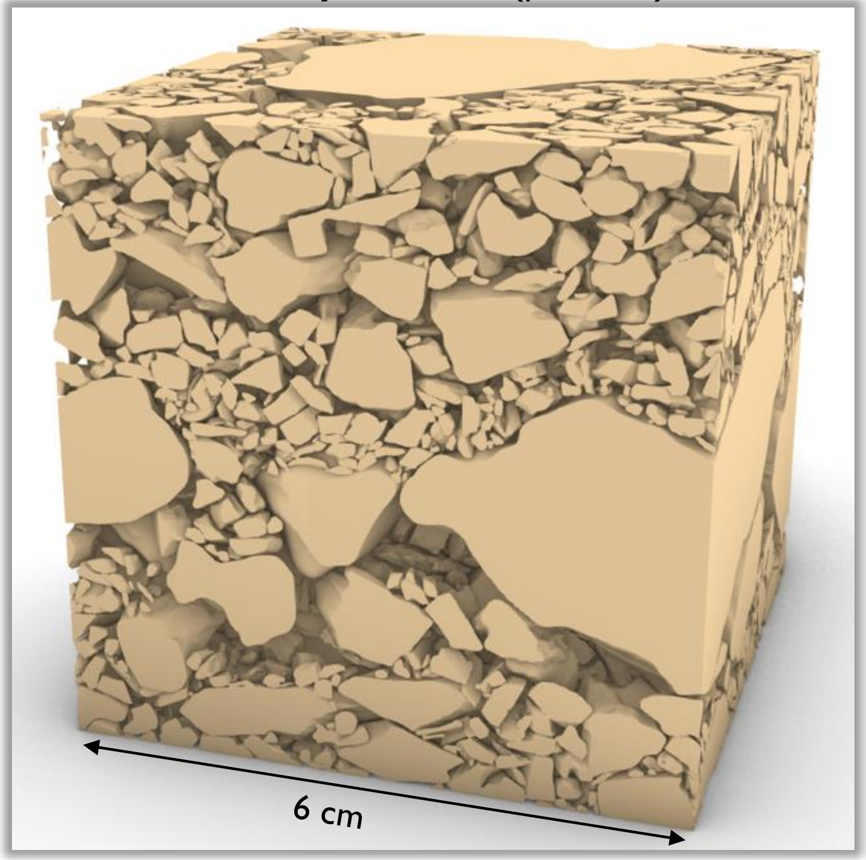

Porosity 26.9 vol% (μ = 0.10 + shaking)

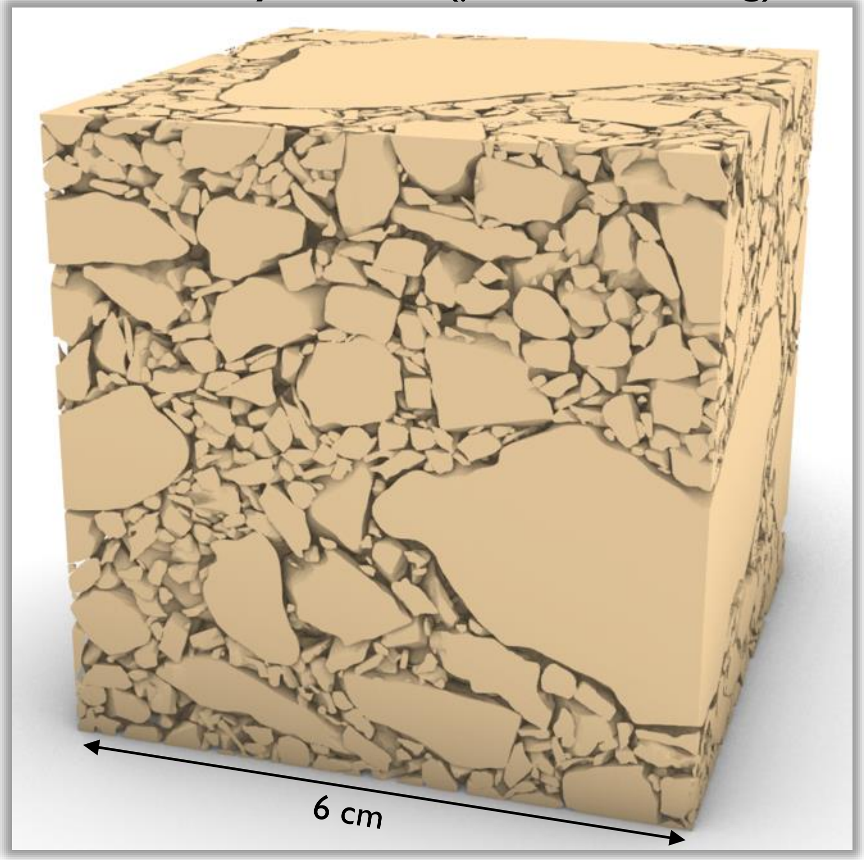

Rubble Deposition Simulations

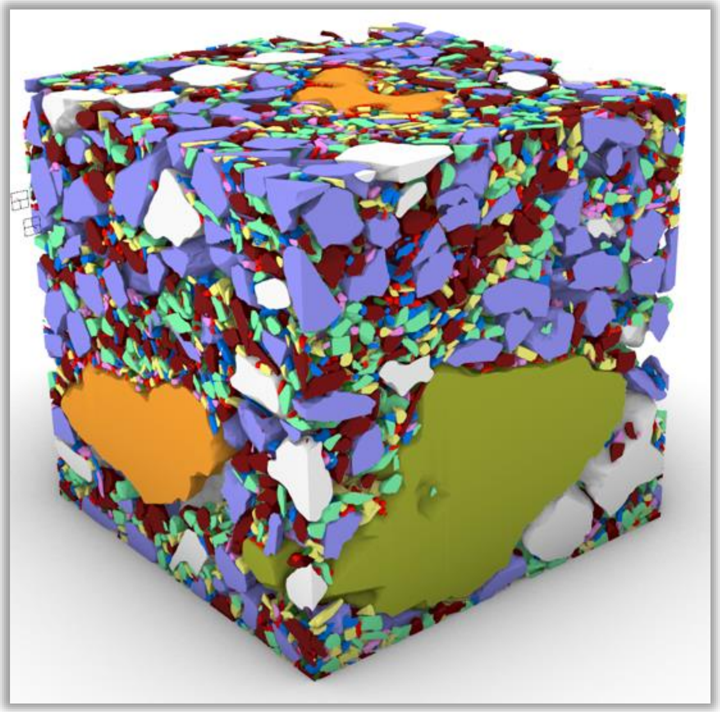

Run Configuration	Friction Coefficient	Porosity, vol%
Gentle	0.77	37.4
Mass dump	0.77	37.0
Shake	0.77	33.6
Mass dump	0.66	34.6
Mass dump	0.58	34.8
Shake	0.10	26.9

UNIFORM (MONODISPERSE) VS. SIEVE SIZE DISTRIBUTIONS (POLYDISPERSE)

Why Variations in Clast Sizes Impacts Depositional Porosity

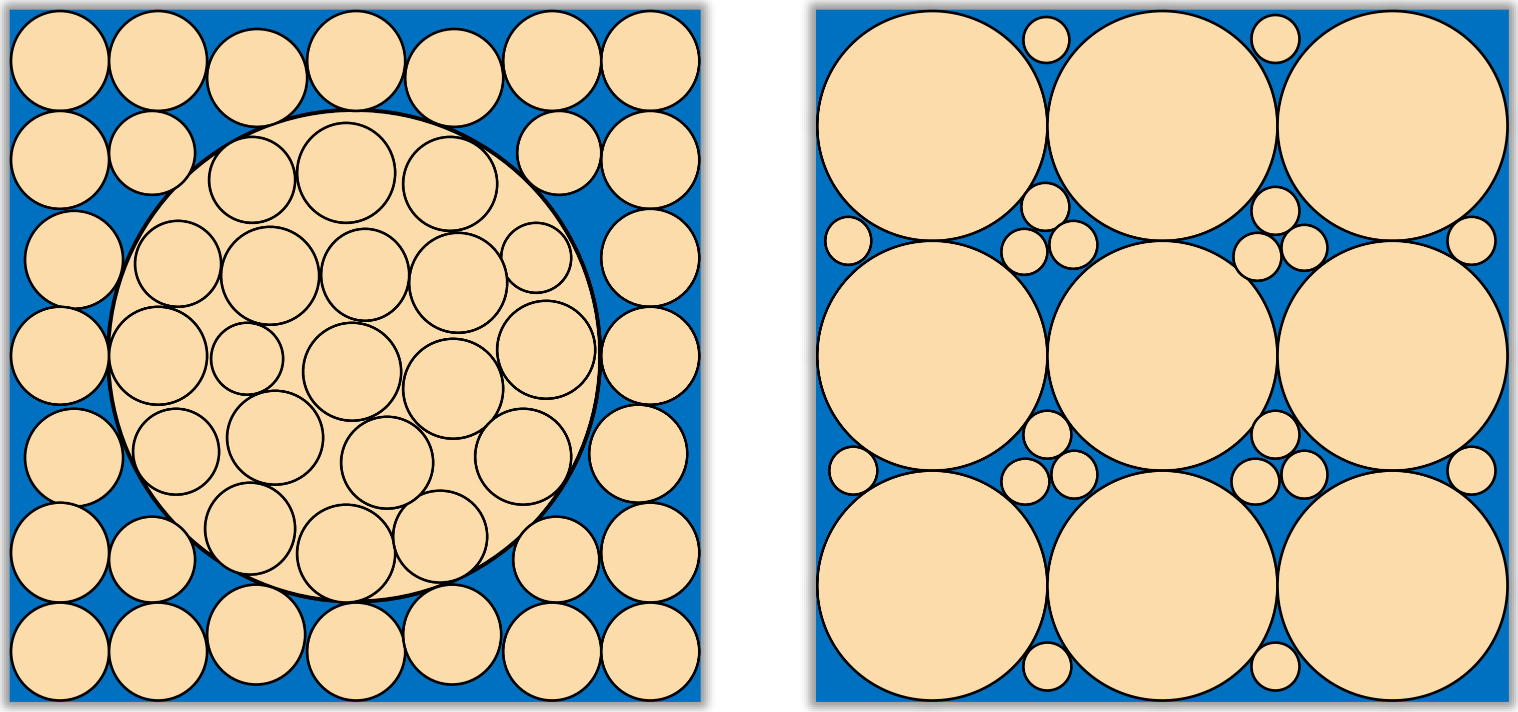

Uniform (Monodisperse) Simulations

Sieve 8 (2.4 – 3.4 mm)

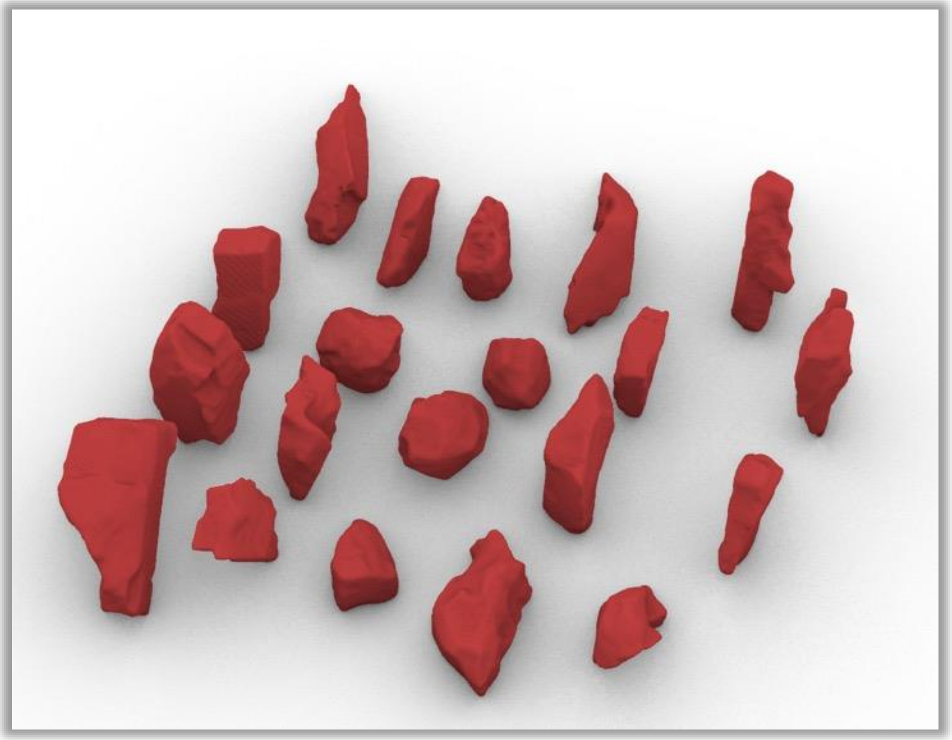

Size: 2.88 mm

- mid point for sieve 8 fraction

Sieve 8 shapes

- Scaled so that minimum sieve pass through size = 2.88 mm

Friction coefficient = 0.77

Mass dump deposition mode

μCT Shapes: Uniform vs. Sieve Size Distribution ($\mu = 0.77$)

Porosity 47.0 vol%

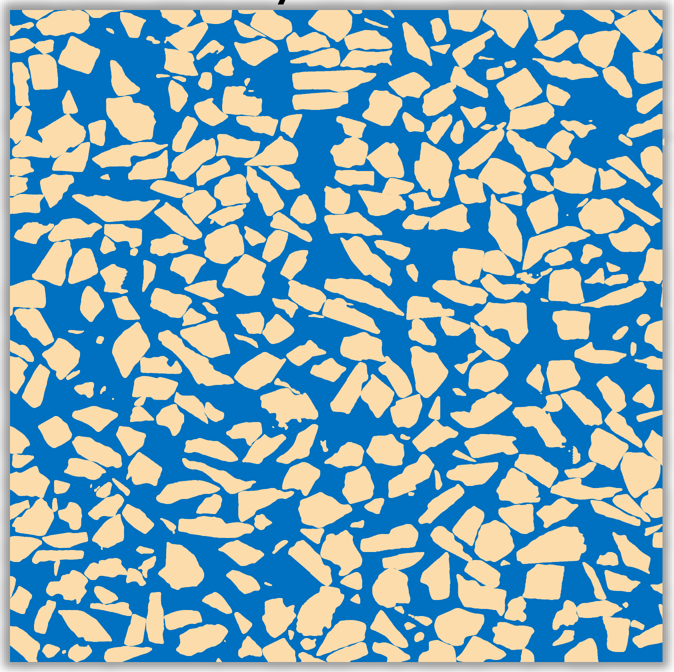

Porosity 37.0 vol%

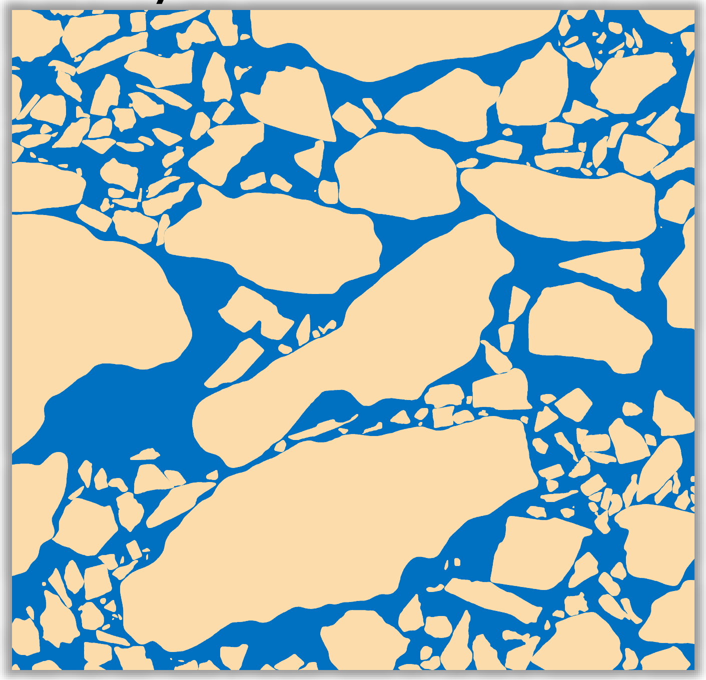

Permeability calculations will tell us how important these differences are, e.g. are the porosity-permeability surfaces different based on size distribution

SPHERES VS. μCT SHAPES

Clast Deposition Simulations: Summary

Mode	Clast Shape	Size Distribution	Friction Coef.	Porosity, vol%
Gentle deposition	μCT scans	WIPP Sieve	0.77	**37.37**
Mass dump	μCT scans	WIPP Sieve	0.77	**37.04**
Shake	μCT scans	WIPP Sieve	0.77	33.62
Mass dump	μCT scans	WIPP Sieve	0.66	34.56
Mass dump	μCT scans	WIPP Sieve	0.58	34.75
Shake	μCT scans	WIPP Sieve	0.10	26.94
Mass dump	μCT scans	Uniform	0.77	47.73
Mass dump	Sphere	WIPP Sieve	0.77	25.69
Shake	Sphere	WIPP Sieve	0.10	20.03
Mass dump	Sphere	Uniform	0.77	47.73
Shake	Sphere	Uniform	0.77	40.38
Shake	Sphere	Uniform	0.10	36.39

Good agreement with UNM experiments

- Angle of repose
- Δ porosity from shaking

Rubble results

- Best result for initial WIPP conditions: ~37% porosity
- Important variables: clast size distribution, clast shapes, shaking, friction

Monodisperse: Spheres vs. Sieve 8 μCT Shapes

Porosity 47.7 vol%

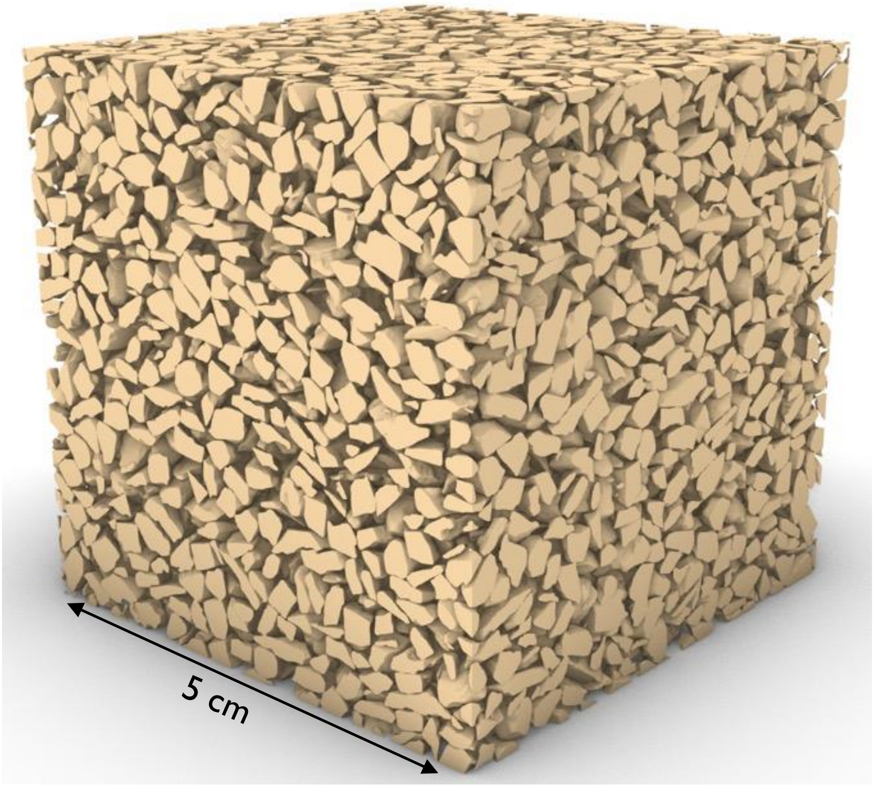

Porosity 40.4 vol%

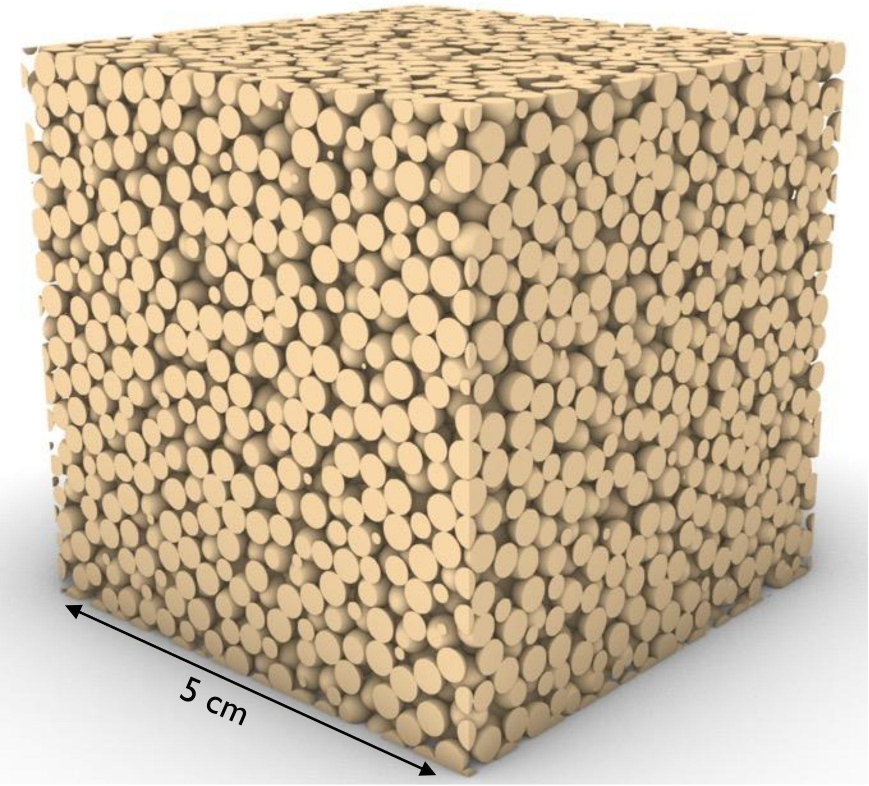

Monodisperse: Spheres vs. Sieve 8 μCT Shapes

Porosity 47.7 vol%

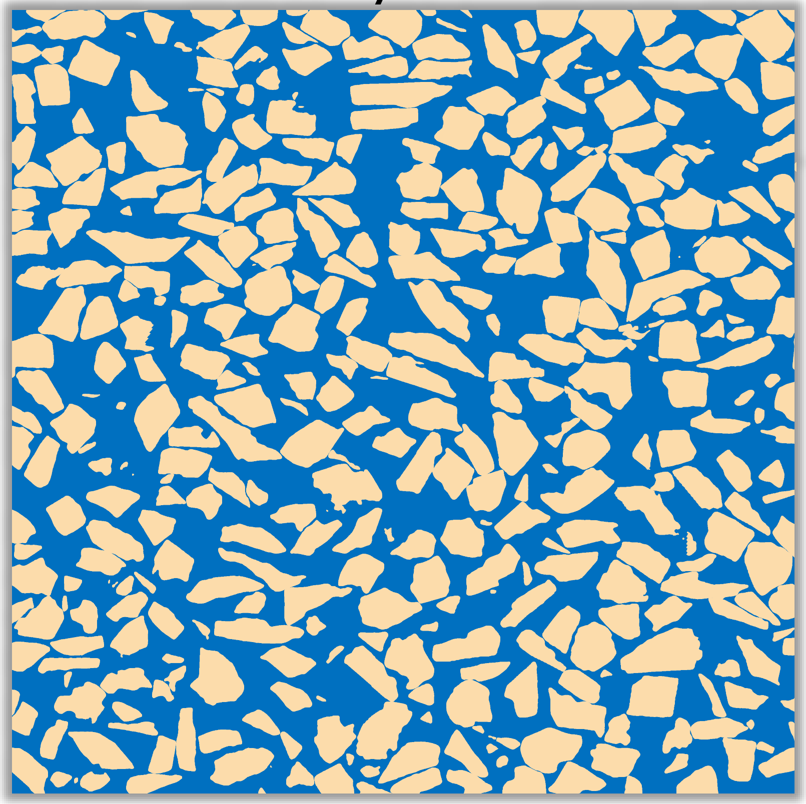

Porosity 40.4 vol%

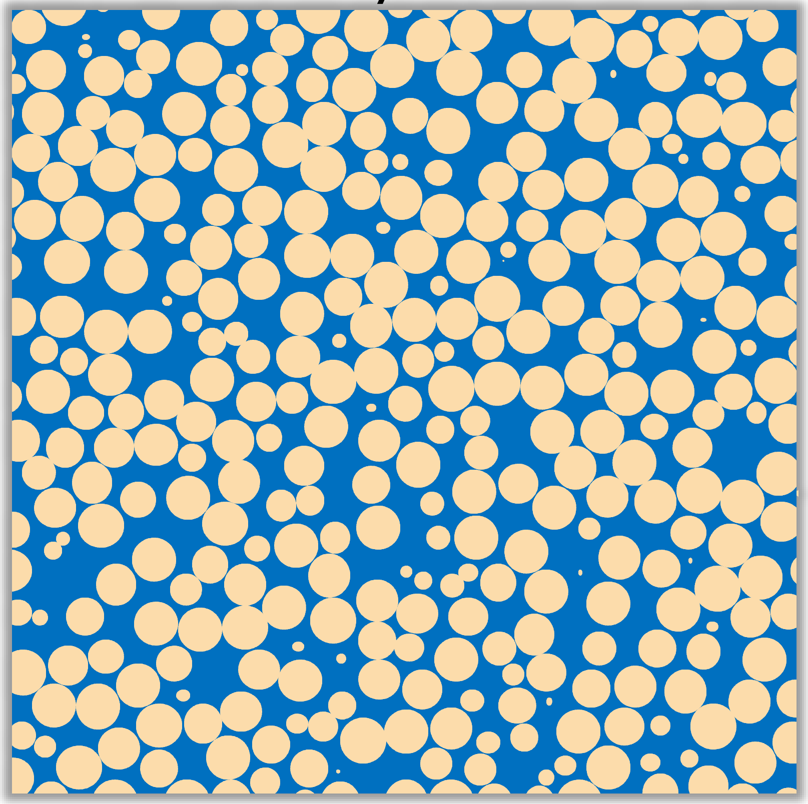

Sieve Size Distribution: Spheres vs. Actual Shapes (μ 0.77)

Porosity 37.0 vol%

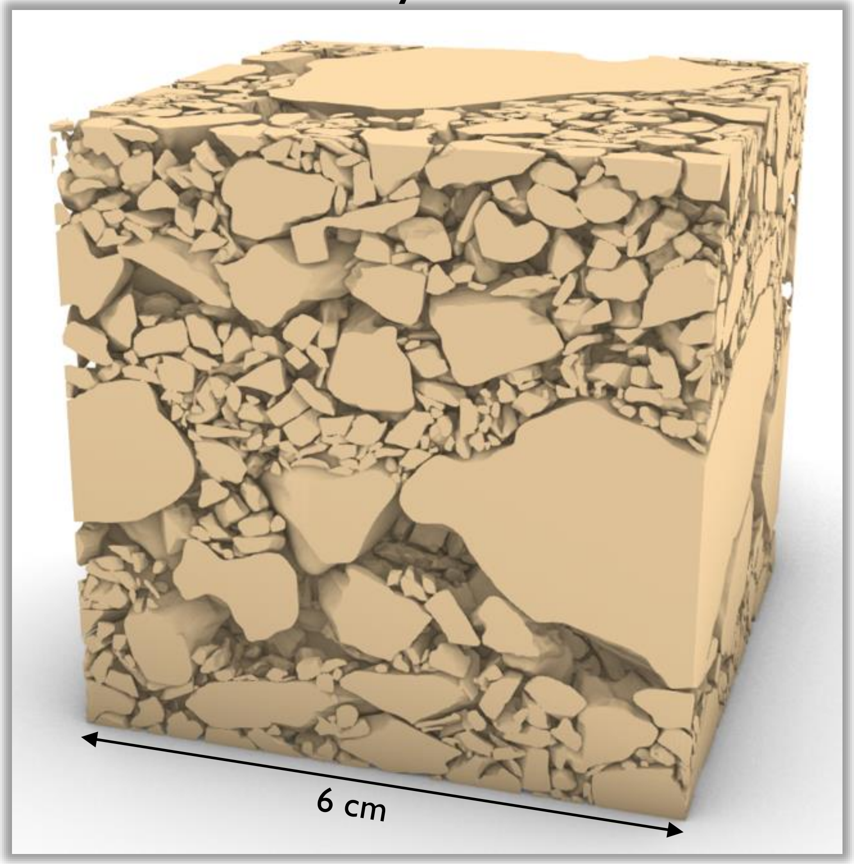

Porosity 25.7 vol%

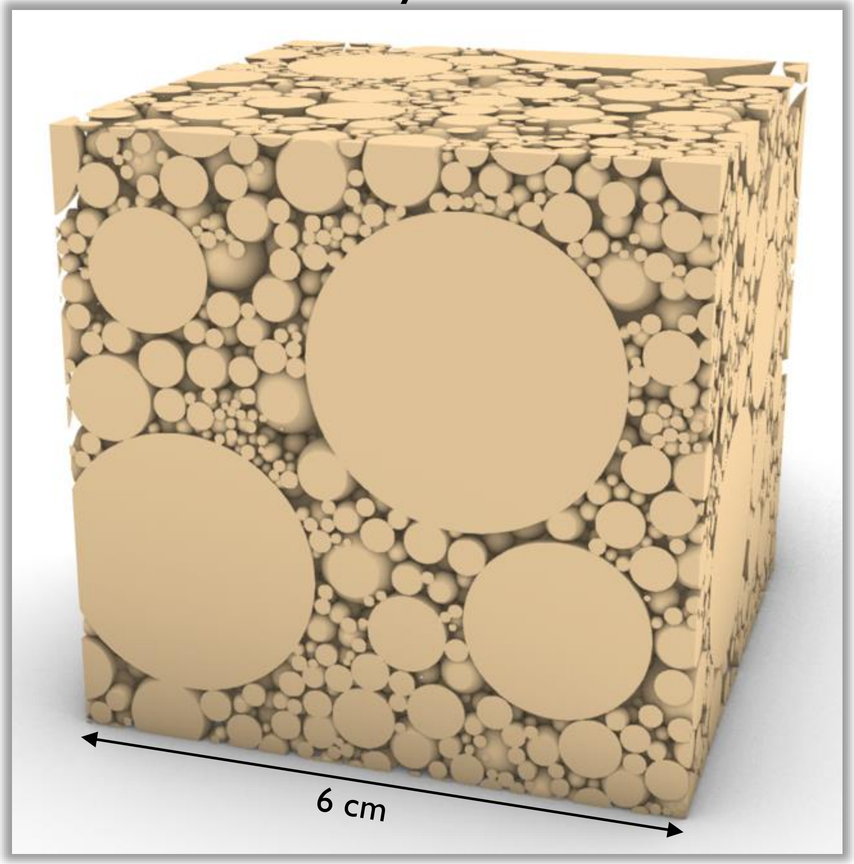

Sieve Size Distribution: Spheres vs. Actual Shapes (μ 0.77)

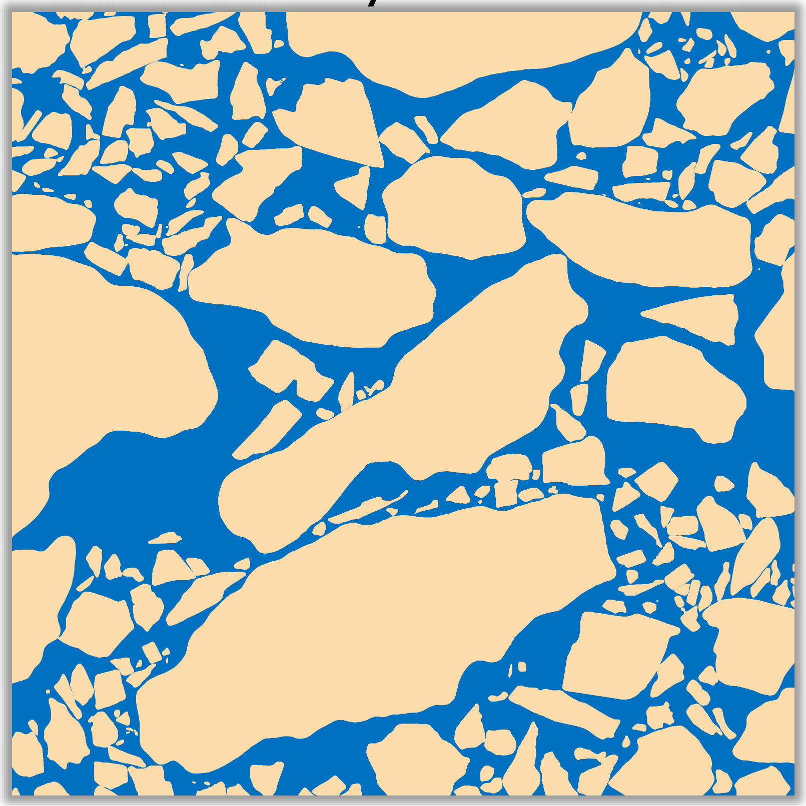

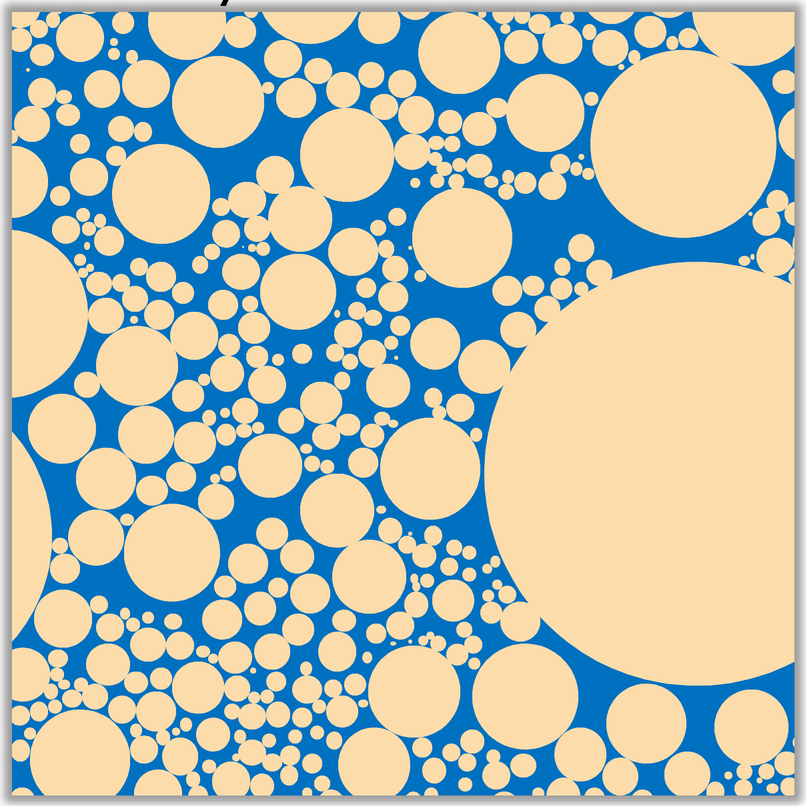

Shape matters w.r.t. porosity -> we have observed that larger fragments tend to be less spherical.

Of course, lower porosity doesn't necessarily equate to lower permeability

MECHANICAL COMPACTION

Uniaxaial Compaction Simulation

1. Salt Behavior
   1. Elasticity
   2. Pressure solution creep
   3. Dislocation creep
   4. No damage or fracturing
2. Uniaxial Strain
   1. Piston on top
   2. Other boundaries rigid

Initial State: 0 MPa
ϕ = 37 %

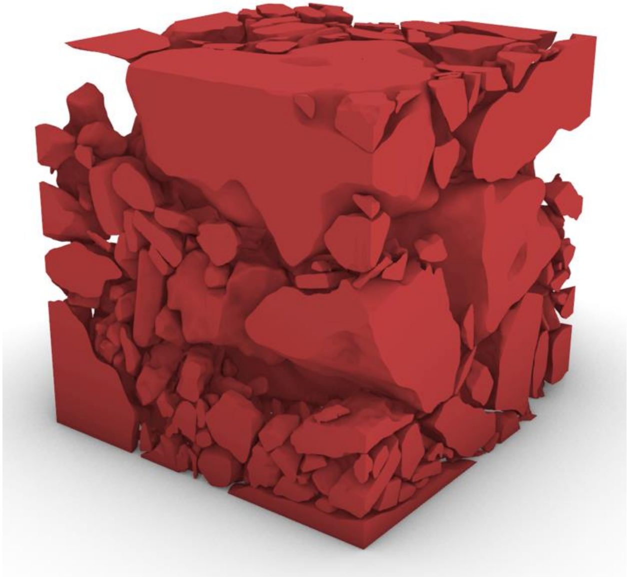

Final State: 15 MPa
ϕ = 6 %

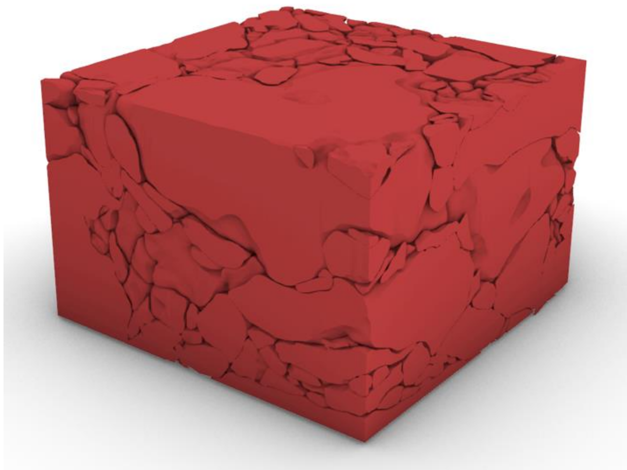

Steady-State CFD Simulation of Air Flow

Clasts

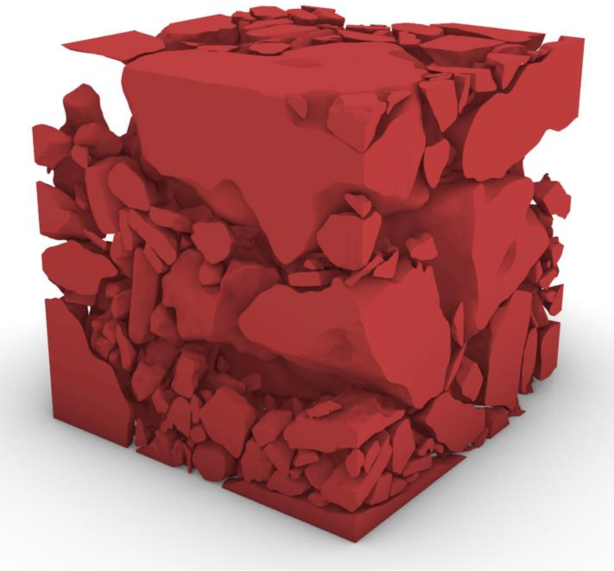

Pore Space

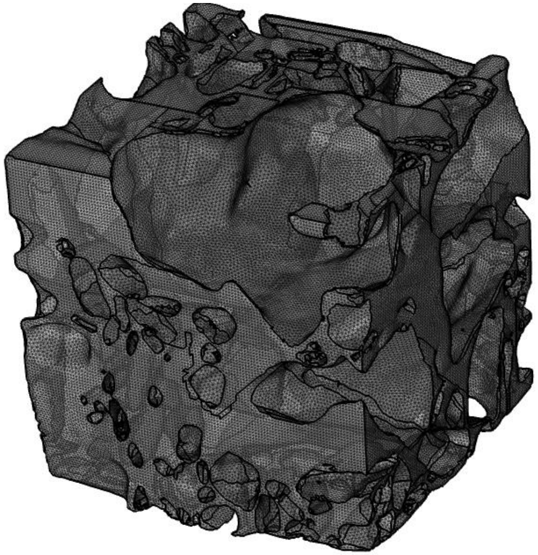

Air Flow Streamlines and Speed (m/s)

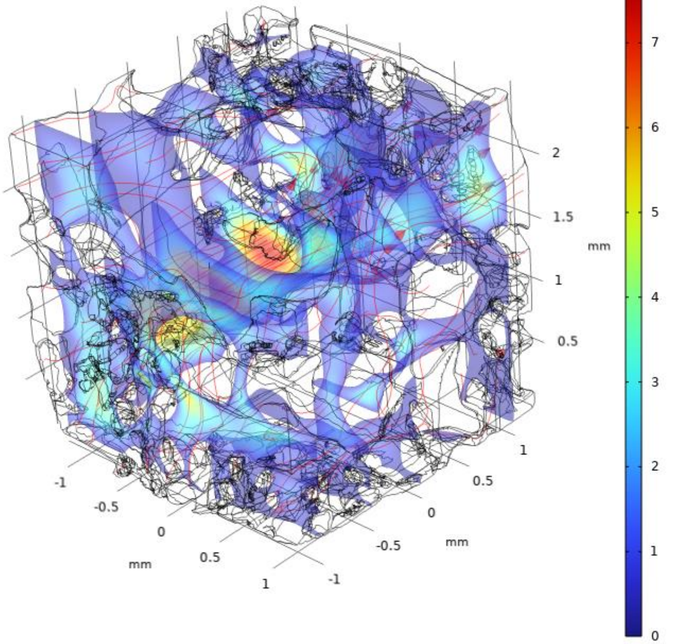

EXPERIMENTAL VALIDATION

1/10th Scale Porosity and Permeability Measurements

Experimental Setup

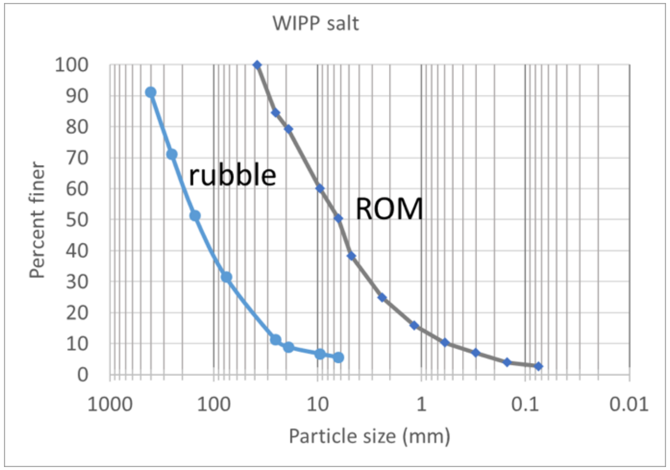

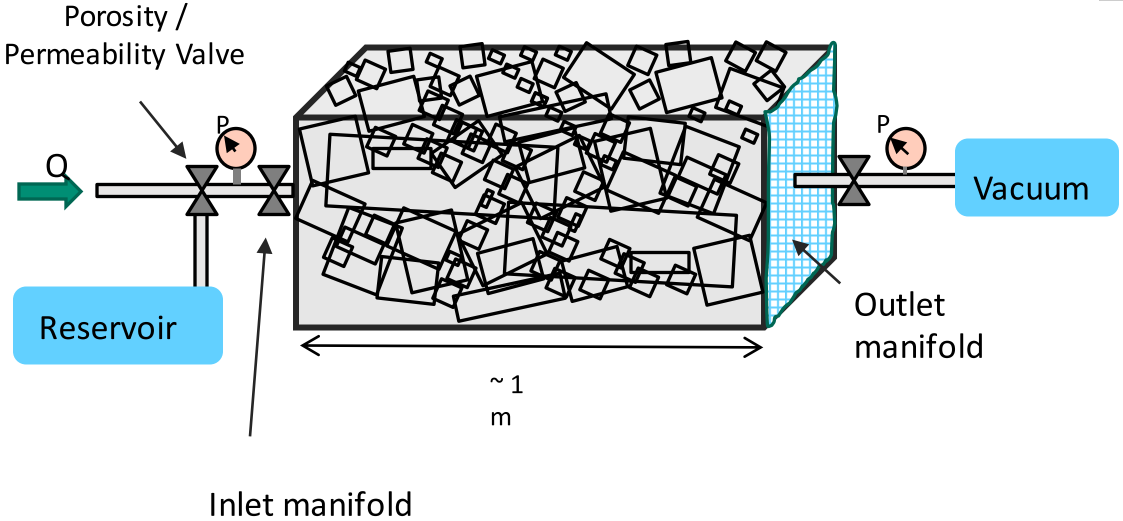

Preliminary Results

	k (m^2)	ϕ (%)
ROM	$5x10^{-9}$	37
Rubble	$3x10^{-8}$	39

Geomechanics Laboratory

Porosity test configuration

Connect reservoir of known volume and pressure to unknown pore volume of salt under vacuum, and then allow to equilibrate. Porosity interpreted from equilibrium pressure.

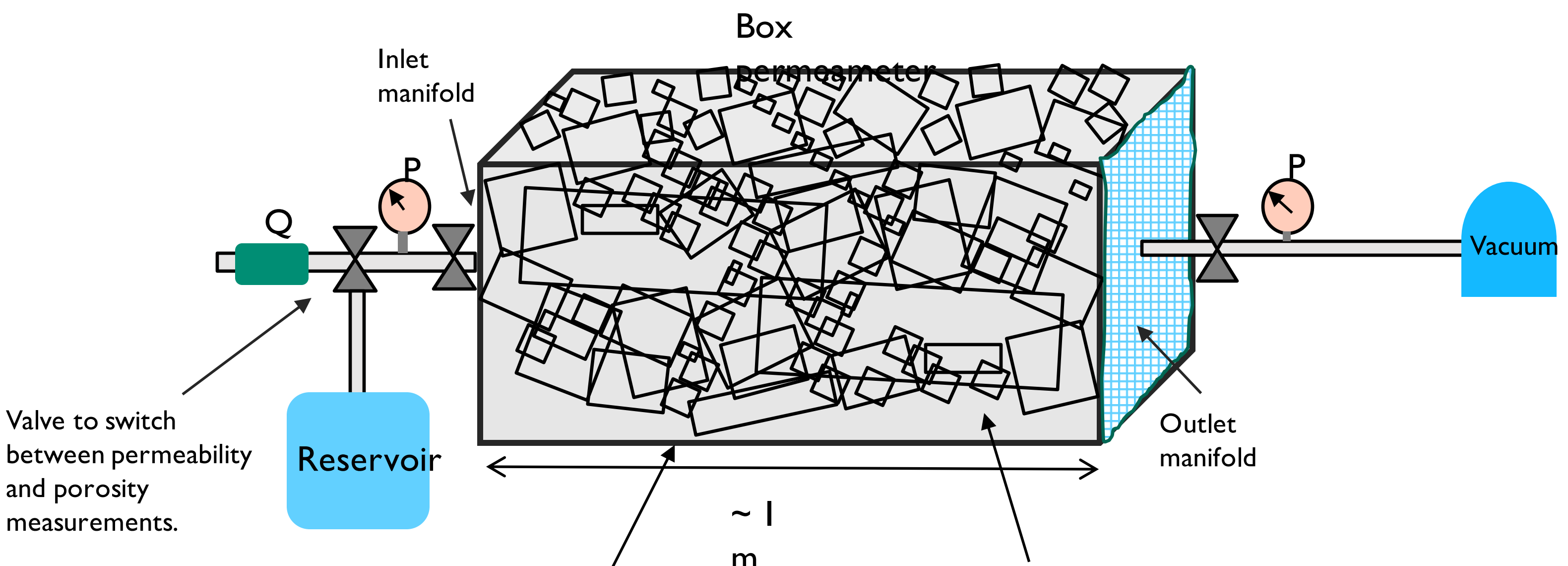

Box is portable. Permeability and porosity measurement systems can be disconnected.

Salt particles contained within plastic liner that serves as jacket for vacuum permeability and porosity measurements.

Geomechanics Laboratory

Permeability test configuration

Vacuum induces flow through salt. Pressure drop (P) and flow rate (Q) measured to interpret permeability.

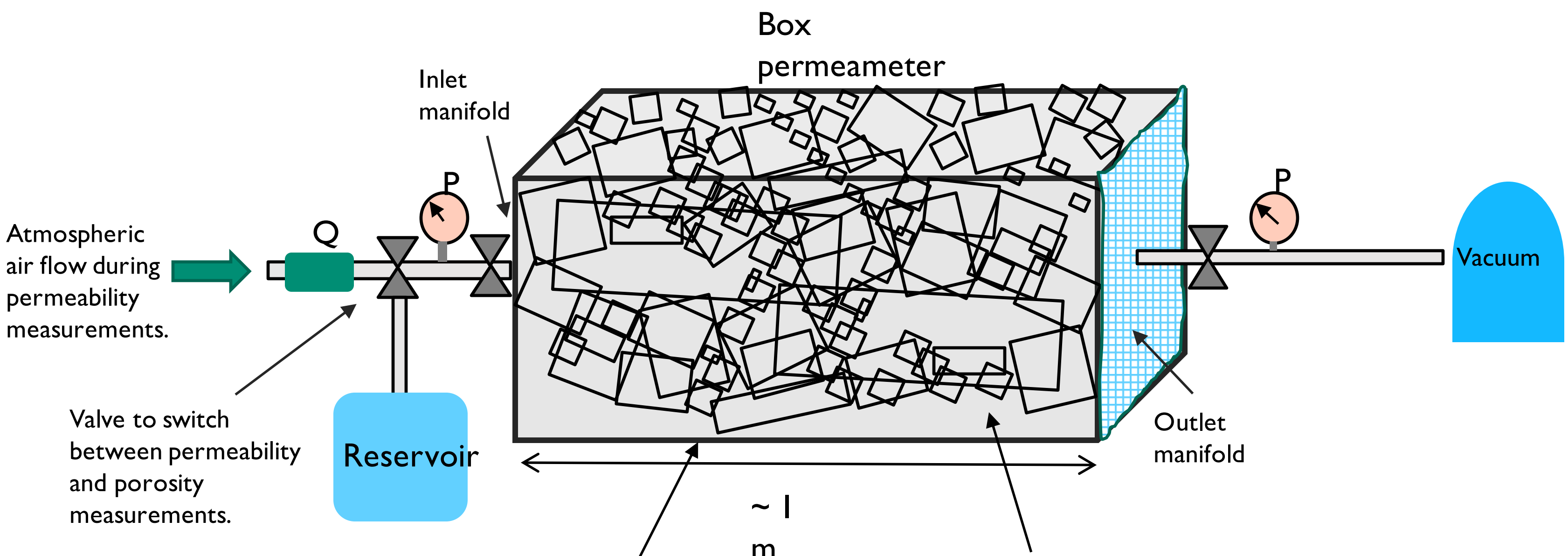

Box is portable. Permeability and porosity measurement systems can be disconnected.

Salt particles contained within plastic liner that serves as jacket for vacuum permeability and porosity measurements.

Two "types" of granular WIPP salt tested: ROM and rubble

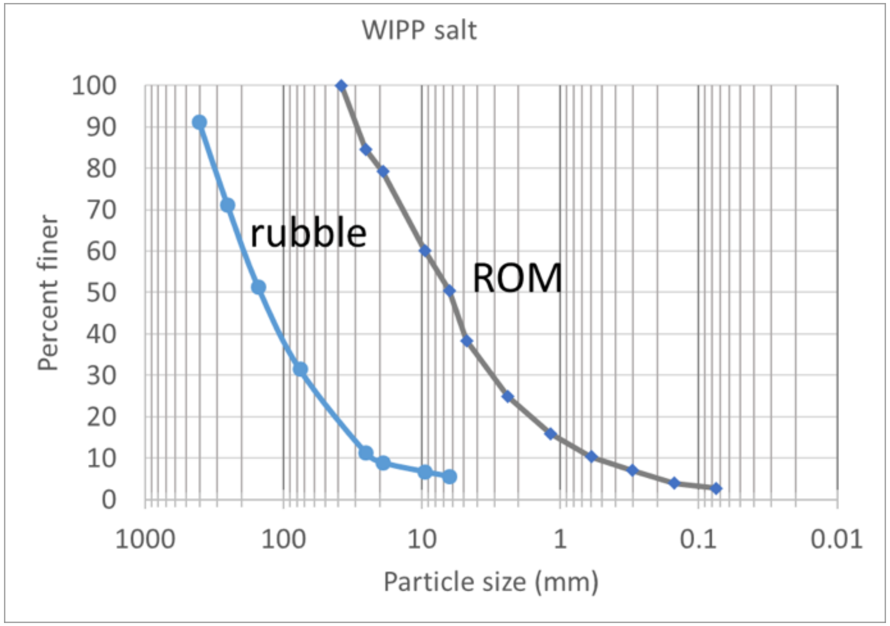

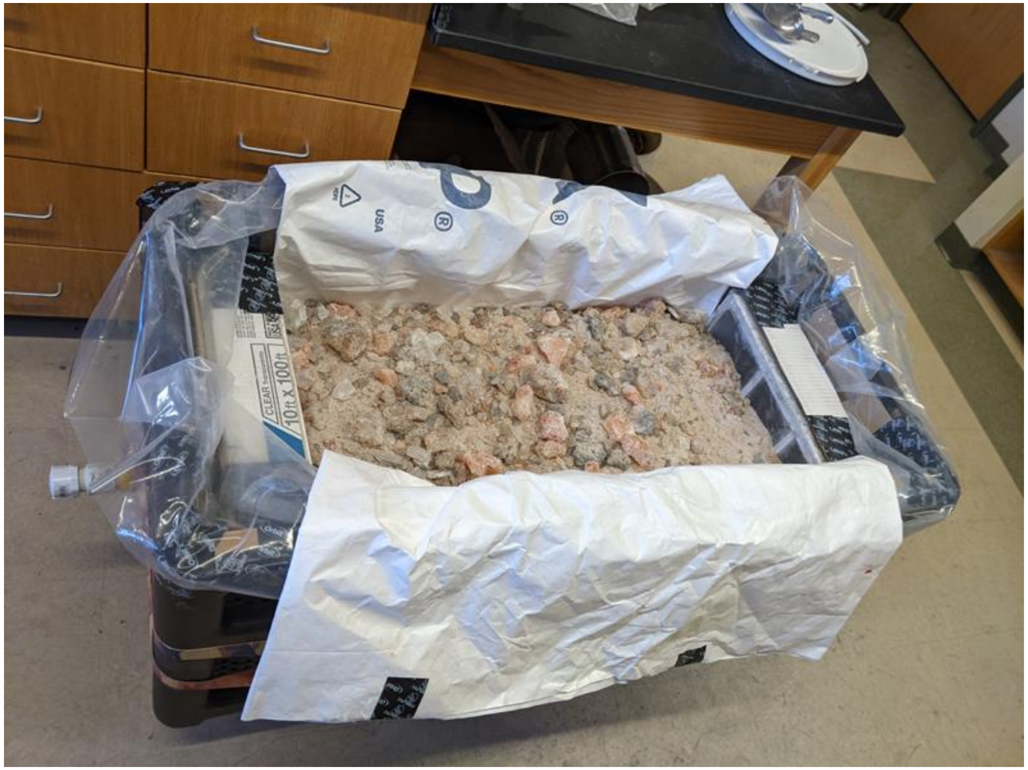
USA
CLEAR
10ft x 100ft

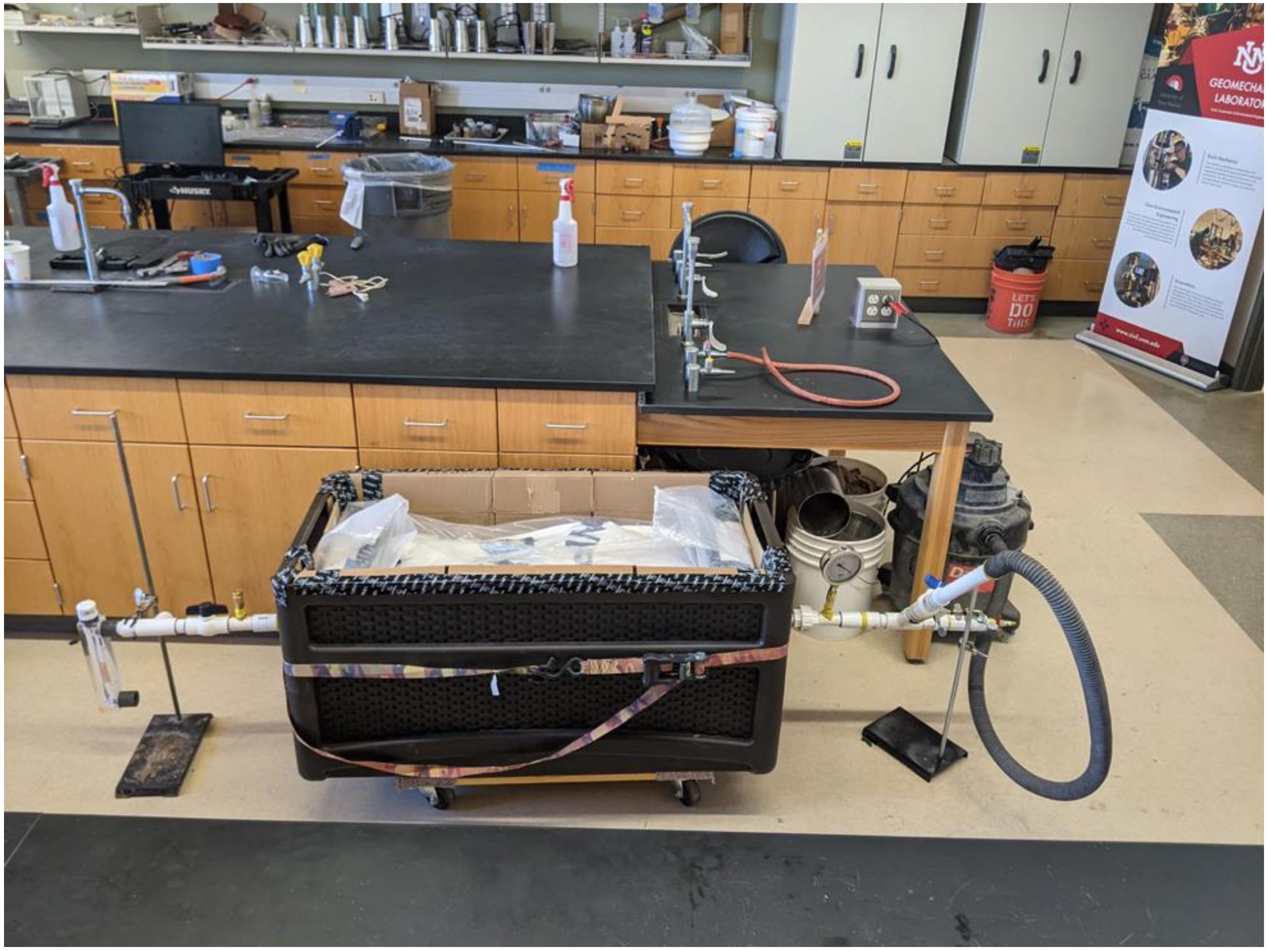

Preliminary Results

	Permeability (m^2)	Porosity (%)
ROM	$5x10^{-9}$	37
Rubble	$3x10^{-8}$	39

Angle of repose measurements on ROM salt

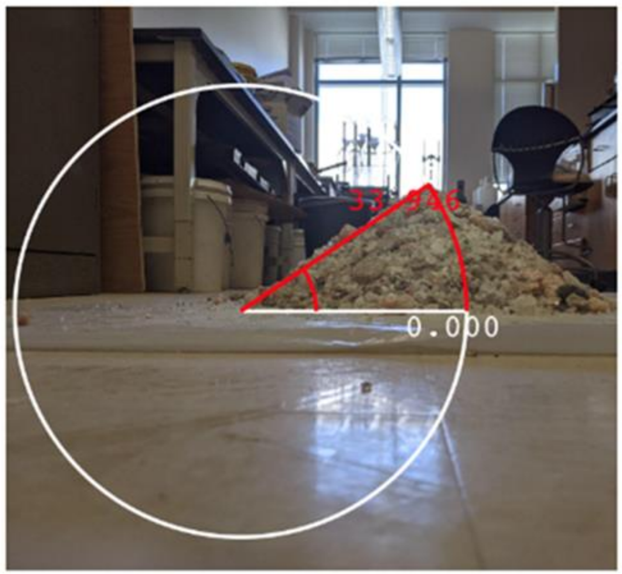

Average from 8 measurements = 35.4°

Summary and Future Work

Summary
- Developed a capability/workflow to examine the effects of particle shape, size, and size distribution on depositional porosity
- Depositional Study shows importance of friction parameter, as well as shape and size distribution
- Angle of repose and study on spherical studies provide some measure of confidence in the depositional methodology
- Shaking tests (both computational and experimental) suggest a good correspondence, and imply that ~3% porosity reduction is possible without mechanical compaction

In Progress:
- Permeability analysis of deposition derived meshes via CFD (*in process)*
- Validation study of 1:10 scale box permeameter using microCT
    - Comparison CFD permeability

    (*Test completed Spring 2022 – post-processing in progress)*
- Mechanical compaction work (*in process*)
    - Biaxial/triaxial stress
    - Viscoplastic deformation
    - Pressure Solution

(Back-up Slides)

Brief Overview of Literature

Key Points:

- Mode of construction
  - Sequential Deposition results in lower porosity than Monte Carlo
  - However, transport depends only on porosity
- Random and homogenous packing

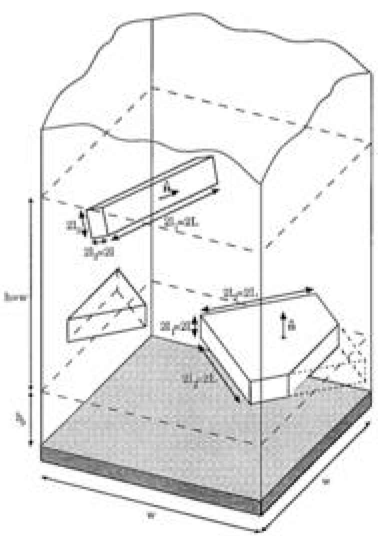

PHYSICAL REVIEW E VOLUME 55, NUMBER 2 FEBRUARY 1997

Geometrical and transport properties of random packings of spheres and aspherical particles

D. Coelho,[1] J.-F. Thovert,[1] and P. M. Adler[2]
[1]*Laboratoire des Phénomènes de Transport dans les Mélanges (LPTM), SP2MI, Bd 3, Téléport 2, F-86960 Futuroscope, France*
[2]*IPGP, tour 24, 4, Place Jussieu, 75252 Paris Cedex 05, France*
(Received 7 March 1996; revised manuscript received 30 September 1996)

Random packings of grains of arbitrary shape are built with an algorithm that is mostly applied to spheres, ellipsoids, cylinders, and parallelepipeds. A systematic account of the main geometrical properties such as the porosity, the reduced specific area, etc. is given. The conductivity, the permeability, and the dispersion are also systematically determined and they are shown not to depend upon their mode of construction.
[S1063-651X(97)13802-8]

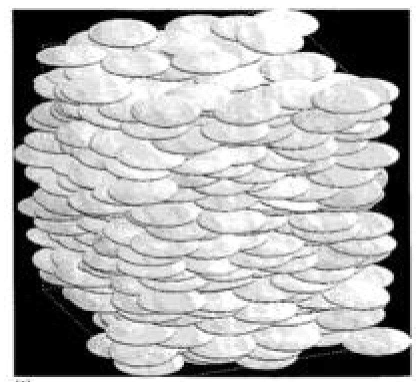

(a)

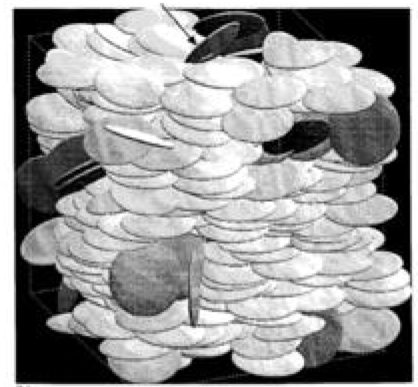

(b)

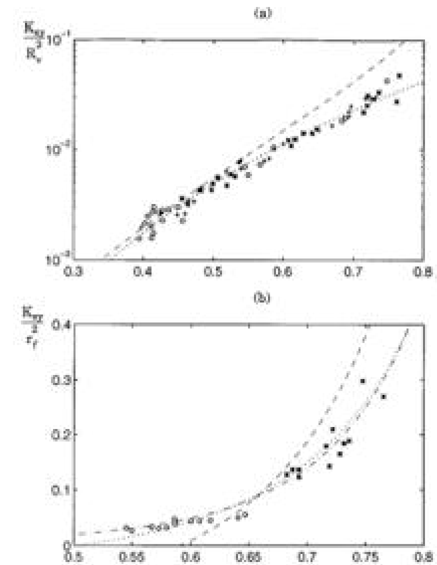

FIG. 15. Permeability as function of porosity. (a) K_{xy}/R_0^2 of random beds of ellipsoids (○), cylinders (+), and parallelepipeds (*) vs the porosity ϵ. The dot is the measurement of Thiess-Weesie *et al.* [34]. The broken line is Eq. (34c) with $k/\Psi^2=10$; the dotted line is the least square fit Eq. (41). (b) The permeability K_{xy}/r_f^2 of random beds of prolate particles with $L/l=5$ (○) and 10 (*) vs the porosity ϵ. The broken line is Eq. (37) with $k_4=6.1$ and $k_5=0.64$. The dotted line is Eq. (37) with $k_4=12.6$ and $k_5=0.707$. The dashed line is Eq. (38).

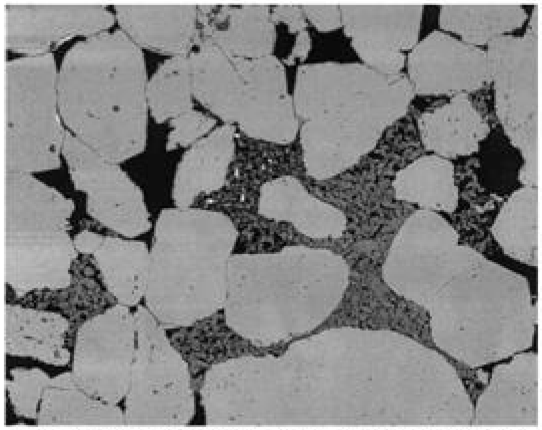

Figure 1. BSE image of a thin section from a North Sea reservoir sandstone. The pore space is black, solid (quartz/feldspar) is light grey, and clay is dark grey.

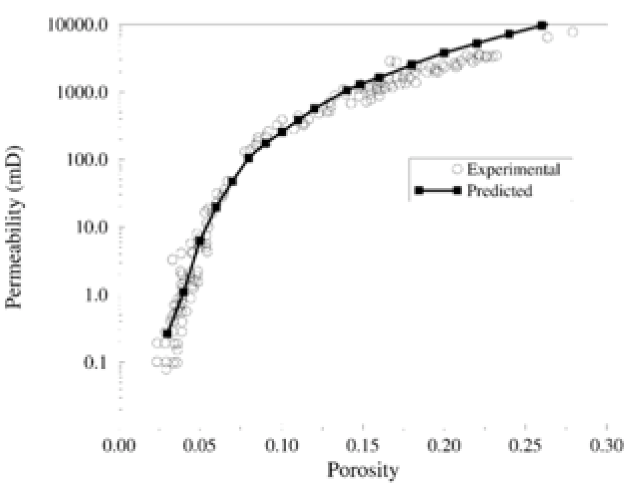

Figure 13. Comparison between measured and computed (directionally averaged) permeabilities of Fontainebleau sandstones.

Transport in Porous Media **46:** 311–343, 2002.

Process Based Reconstruction of Sandstones and Prediction of Transport Properties

PÅL-ERIC ØREN and STIG BAKKE
Statoil Research Centre, N-7005 Trondheim, Norway

Abstract. We present a process based method for reconstructing the full three-dimensional microstructure of sandstones. The method utilizes petrographical information obtained from two-dimensional thin sections to stochastically model the results of the main sandstone forming processes – sedimentation, compaction, and diagenesis. We apply the method to generate Fontainebleau sandstone and compare quantitatively the reconstructed microstructure with microtomographic images of the actual sandstone. The comparison shows that the process based reconstruction reproduces adequately important intrinsic properties of the actual sandstone, such as the degree of connectivity, the specific internal surface, and the two-point correlation function. A statistical reconstruction of Fontainebleau sandstone that matches the porosity and two-point correlation function of the microtomography data differs strongly from the actual sandstone in its connectivity properties. Transport properties of the samples are determined by solving numerically the local equations governing the transport. Computed permeabilities and formation factors of process based reconstructions of Fontainebleau sandstone compare well with experimental measurements over a wide range of porosity.

Key words: 3D reconstruction, microstructure, Fontainebleau sandstone, percolation, permeability, formation factor.

PHYSICAL REVIEW E **80**, 021304 (2009)

Numerical study of the effects of particle shape and polydispersity on permeability

Xavier Garcia,[1,*] Lateef T. Akanji,[1,†] Martin J. Blunt,[1,‡] Stephan K. Matthai,[2,§] and John Paul Latham[1,‖]
[1]*Department of Earth Science and Engineering, Imperial College London, SW72AZ London, United Kingdom*
[2]*School of Petroleum Engineering, Montanuniversität, Max-Tendler-Strasse, A-8700, Leoben, Austria*
(Received 11 May 2009; published 26 August 2009)

We study through numerical simulations the dependence of the hydraulic permeability of granular materials on the particle shape and the grain size distribution. Several models of sand are constructed by simulating the settling under gravity of the grains; the friction coefficient is varied to construct packs of different porosity. The size distribution and shapes of the grains mimic real sands. Fluid flow is simulated in the resulting packs using a finite element method and the permeability of the packs is successfully compared with available experimental data. Packs of nonspherical particles are less permeable than sphere packs of the same porosity. Our results indicate that the details of grain shape and size distribution have only a small effect on the permeabilty of the systems studied.

DOI: 10.1103/PhysRevE.80.021304 PACS number(s): 45.70.−n, 91.60.Np, 47.56.+r, 47.11.−j

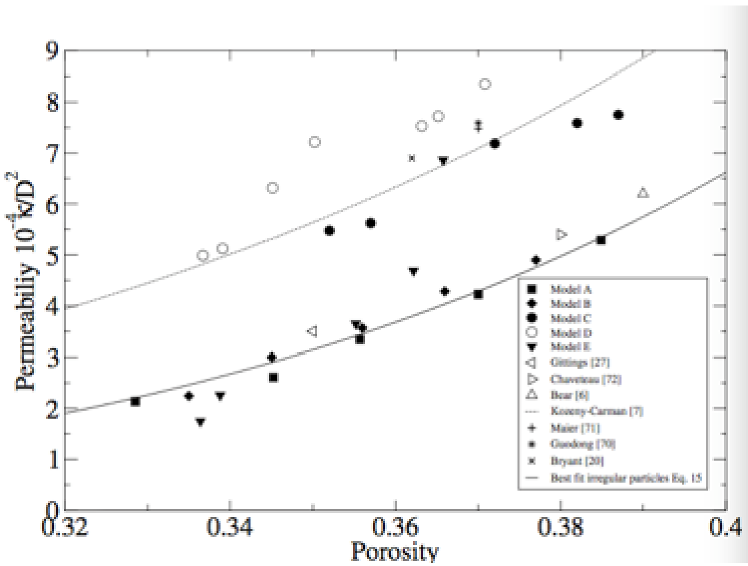

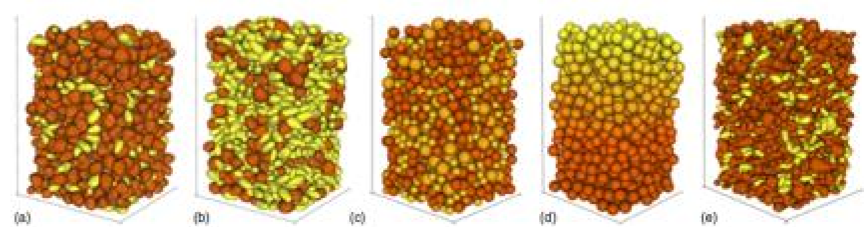

FIG. 4. (Color online) *A*: model *A* of a relatively homogeneous sand with semispherical grains. *B*: model *B*, as the previous model but a large number of grains were replaced by elongated grains (light colors). *C*: model *C*, spheres with the same size distribution as in *A*, *B*. *D*: single size spheres. *E*: more heterogeneous sample constructed with a mixture of irregular shapes.

CLAST LIBRARY

Clast Library

Create collision hulls for clast 3D shapes derived from μCT scans

- Needed for deposition simulations

Relate clast dimensions to sieve opening size

- Clasts' long axes are larger than the opening of sieves that retain them

Rudimentary analysis of clast 3D shapes as a function of size

Size Range for Sieve Opening: 19 - 38 mm

First number
smallest sieve pass through size in mm

Second number
long axis in mm

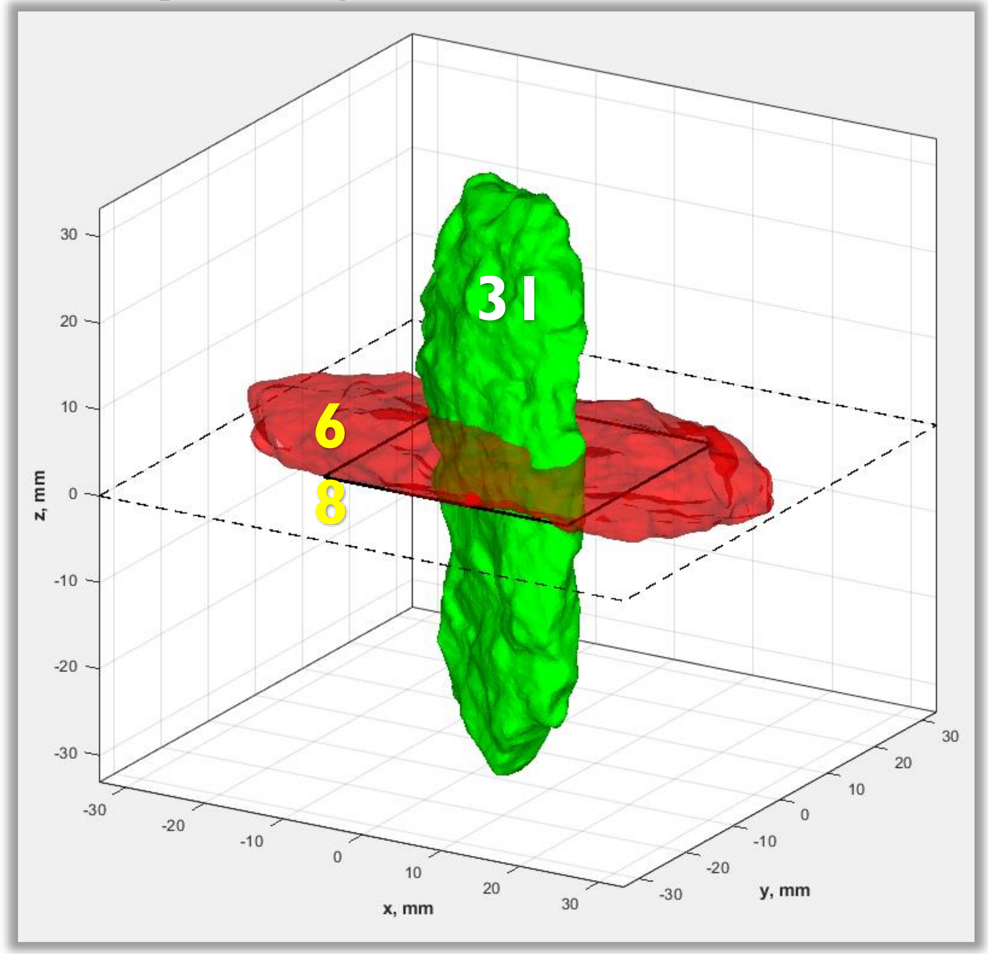

Shape Metrics

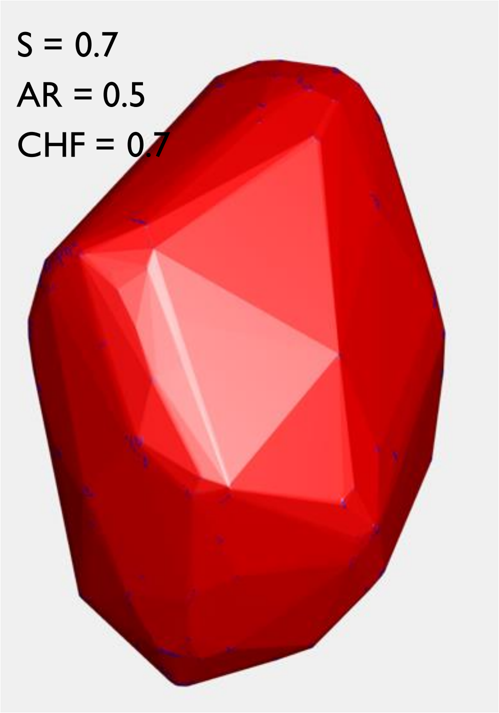

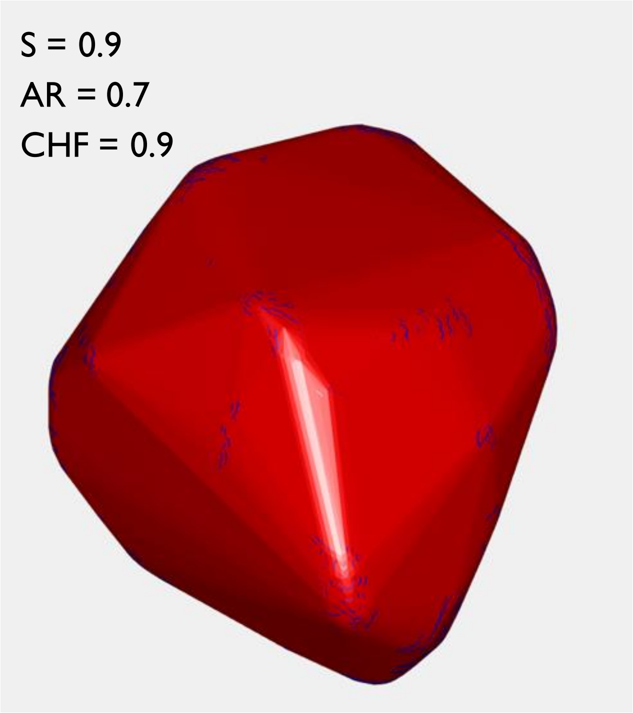

Sphericity
- Area for equal volume sphere / area

Aspect Ratio
- Minimum Ferret length / long axis

Convex hull fill
- Volume / Convex hull volume

Salt Clast Shape Metrics

	Opening, mm		
	Min	Max	Color
Sieve A	38.1	76.2	
Sieve B	19.1	38.1	
Sieve C	9.5	19.1	
Sieve 4	4.7	9.5	
Sieve 6	3.4	4.7	
Sieve 8	2.4	3.4	
Sieve 10	2.0	2.4	
Sieve 12	1.7	2.0	
Sieve 14	1.4	1.7	
Sieve 16	1.2	1.4	
Sieve 18	1.0	1.2	

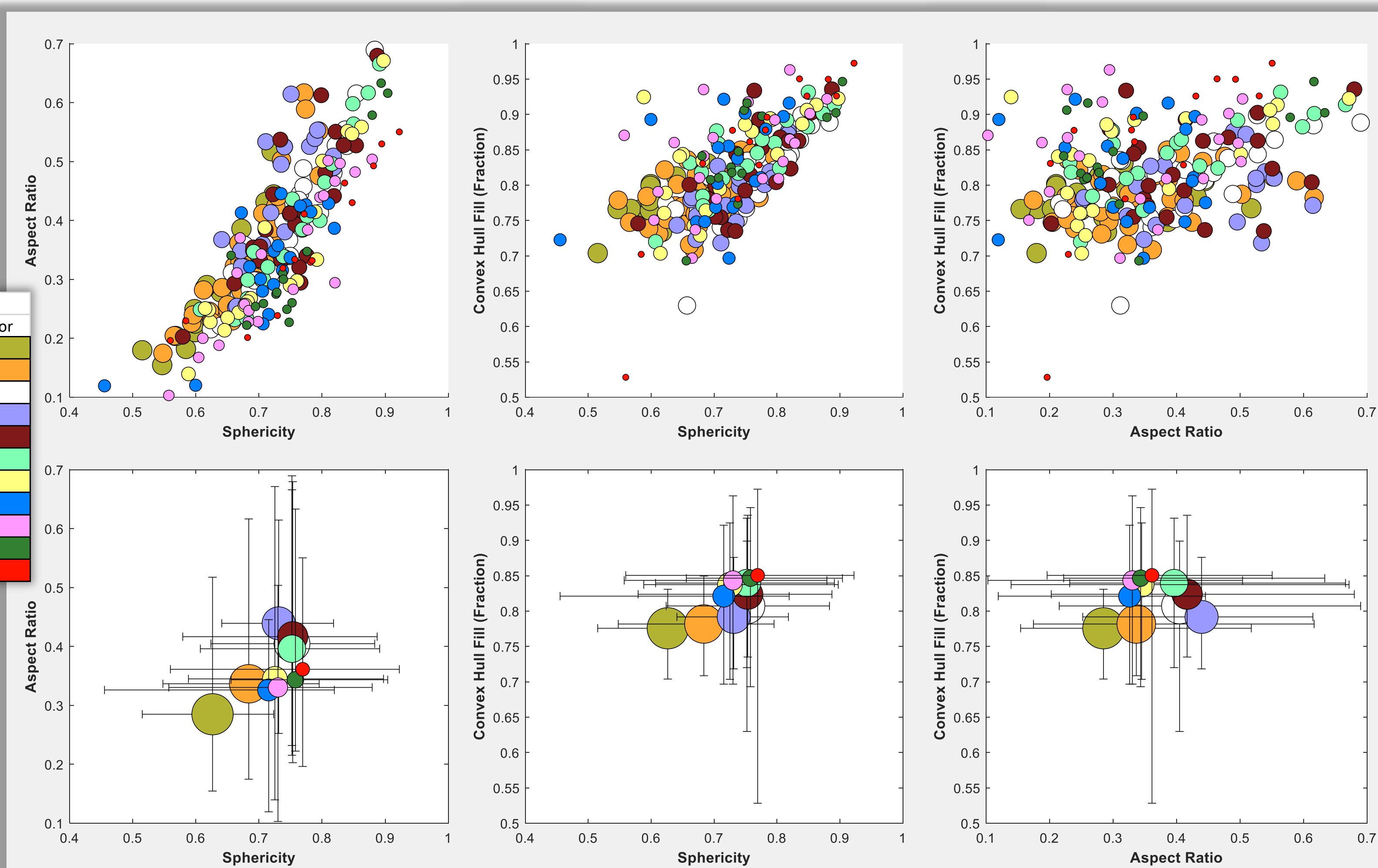

Sieve 19 - 38 mm

First number smallest sieve pass through size in mm

Second number long axis, mm

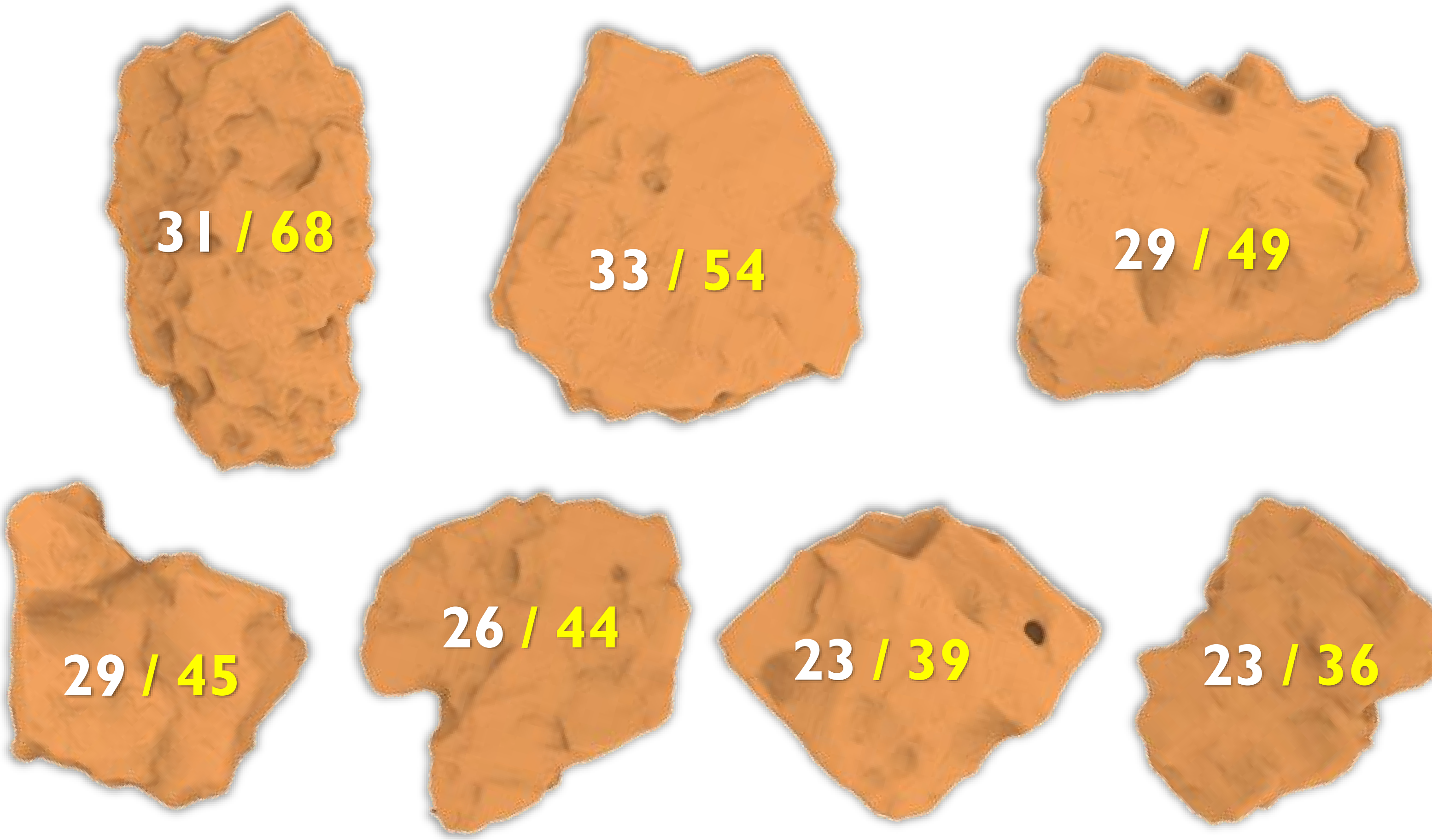

Clast Size from Shape Analysis vs. Sieve Opening Size